Hyaluronan in mesenchymal stromal cell lineage differentiation from human pluripotent stem cells: Application in serum free culture

Paul A De Sousa (paul.desousa@ed.ac.uk)
The University of Edinburgh Centre for Clinical Brain Sciences https://orcid.org/0000-0003-0745-2504
Leo Perfect
National Institute for Biological Standards and Control Division of Biotherapeutics
Jinpei Ye
Shanxi University
Kay Samuels
SNBTS: Scottish National Blood Transfusion Service
Ewa Piotrowska
University of Gdansk: Uniwersytet Gdanski
Martin Gordon
National Institute for Biological Standards and Control Division of Biotherapeutics
Elsa Abranches
National Institute for Biological Standards and Control Division of Biotherapeutics
Thomas M Wishart
The University of Edinburgh The Roslin Institute
David H Dockrell
University of Edinburgh MRC Centre for Inflammation Research: The University of Edinburgh Centre for Inflammation Research
Aidan Courtney
Stroma Therapeutics
Ryan Mate
National Institute for Biological Standards and Control Division of Biotherapeutics

Research Article

Keywords: Pluripotent, Human Pluripotent Stem Cells, Mesenchymal Stromal Cells, Hyaluronan, Cell Therapy

Posted Date: November 7th, 2023

DOI: https://doi.org/10.21203/rs.3.rs-3433788/v1

Abstract

Background

Hyaluronan (HA) is an extracellular glycosaminoglycan polysaccharide with widespread roles throughout development and in healthy and neoplastic tissues. In pluripotent stem cell culture it can support both stem cell renewal and differentiation. However, responses to HA in culture are influenced by interaction with a range of cognate factors and receptors including components of blood serum supplements, which alter results. These may contribute to variation in cell batch production yield and phenotype as well as heighten the risks of adventitious pathogen transmission in the course of cell processing for therapeutic applications.

Main

Here we characterise differentiation of a human embryo/pluripotent stem cell derived Mesenchymal Stromal Cell (hESC/PSC-MSC)-like cell population by culture on a planar surface coated with HA in serum-free media qualified for cell production for therapy. Resulting cells met minimum criteria of the International Society for Cellular Therapy for identification as MSC by expression of. CD90, CD73, CD105, and lack of expression for CD34, CD45, CD14 and HLA-II. They were positive for other MSC associated markers (ie.CD166, CD56, CD44, HLA 1-A) whilst negative for others (eg. CD271, CD71, CD146). In vitro co-culture assessment of MSC associated functionality confirmed support of growth of hematopoietic progenitors and inhibition of mitogen activated proliferation of lymphocytes from umbilical cord and adult peripheral blood mononuclear cells, respectively. Co-culture with immortalized THP1 monocyte derived macrophages (M) concurrently stimulated with lipopolysaccharide as a pro-inflammatory stimulus, resulted in a dose dependent increase in pro-inflammatory IL6 but negligible effect on TNFα. To further investigate these functionalities, a bulk cell RNA sequence comparison with adult human bone marrow (hBM) derived MSC and hESC substantiated a distinctive genetic signature more proximate to the former.

Conclusion

Cultivation of human pluripotent stem cells on a planar substrate of HA in serum-free culture media systems is sufficient to yield a distinctive mesenchymal stromal cell lineage with prospective therapeutic utilities for tissue morphogenesis and repair.

Background

Hyaluronan (also known as Hyaluronate or Hyaluronic Acid; HA) is a broadly distributed glycosaminoglycan (GAG) polysaccharide, comprised of repeating disaccharides of glucuronic acid and N-acetylglucosamine monomers. Extracellularly, its biophysical properties can manifest as a porous

visceoelastic mesh-like structure vital to the physiological function of adult tissue such as cartilage and vitreous humour. This porosity also creates the space necessary for cell migration during embryogenesis, organogenesis, wound repair, tumour metastasis and immune defence. It also functions as a micro environmental cue within tissue niches that co-regulates cell behaviour in these contexts the manner of which depends on its size and availability of cognate factors and receptors (reviewed by Toole, 2004).

HA is synthesized by synthases embedded in the inner leaflet of surface plasma membranes and deposited in the extracellular space, after which it can be internalised and distributed within intracytoplasmic and nuclear compartments. It is cleaved by hyaluronidases resulting in availability in biological fluids and tissues as a spectrum of high molecular weight species (1000–8000 kDA) to smaller molecular weight fragments (< 200 kDa). It is not modified by sulfate groups and is not naturally covalently bound to core proteins as for proteoglycans (Cowman et al., 2015). HA modulation of cell behaviour is mediated by binding to specific hyaluronan binding protein receptors (ie. hyaladhereins) on cell surfaces or within the extracellular matrix (ECM). These include CD44, LYVE-1, HARE, Layilin, RHAMM and TLR4 on the cell surface and aggrecan in the ECM. Binding transduces a range of intracellular signals capable of influencing cell proliferation, energy production, survival, motility, drug resistance and tissue morphogenesis (reviewed in Solis et al., 2012). Tissue specific and conserved effects of HA on stem cell behaviour within niches as well as tissue morphogenesis have been described for haematopoiesis, cardiogenesis, osteogenesis chondrogenesis, neurogenesis and angiogenesis (reviewed in Zoller, 2015, Bonafe et al., 2014; Zhai et al., 2020; Kim et al., 2011; Su et al., 2019, Pardue et al., 2008). As noted these may depend on HA size. For example, in the developing and adult nervous system low molecular weight HA fragments from endogenous ECM cleaved by hyaluronidases or microbial sources can stimulate defensive response pathways via TLR. Stimulation of same with high molecular weight HA promotes cell proliferation and wound repair (Stenson et al., 2021; Peters and Sherman, 2020).

In developing mammalian embryos HA is differentially associated with the inner cell mass vs the trophectoderm, and is a prominent feature of post-implantation embryonic cavities and growing tissues (Brown and Papaioannou, 1993). In culture hESC derived from embryo inner cell mass self-renew when encapsulated in 3 Dimensional (3D) Methylacrylated HA hydrogels in first generation feeder cell-conditioned and knockout serum replacement (KOSR) supplemented media as developed by Xu et al., 2001 (Gerecht et al., 2007). The same has been reported in 3-D culture of hESC in Tyramine-HA hydrogels in next generation molecular defined serum-free media (mTESR1™; Xu et al., 2015). Sulfated, but not non-sulfated HA can preserve undifferentiated colony phenotype in the short term (3 day) absence of bFGF and feeder conditioned medium in 2 D planar culture (Miura et al., 2019). By contrast, we have previously observed that cultivation of hESC on a planar coating of HA in first generation feeder cell conditioned and KOSR supplemented media yielded a proliferative but mortal multi-lineage potent mesenchymal stromal cell (MSC)-like lineage biophysically distinct from hESC and other differentiated cells (De Sousa 2012; Velugotla et al., 2012). Augmentation of this culture system with fetal calf serum also yields an MSC-like lineage and osteogenic potential (Harkness et al., 2011). Whilst media supplementation with blood serum is common, its usage in the manufacturing of cells for clinical application heightens potential for variation in cell batch production and risk of adventitious pathogen transmission (De Sousa et al., 2019).

Here we revisited hESC cultivation on a planar substrate of HA as a route to differentiation of MSC-like cells from pluripotent hESC this time using state of the art serum-free culture systems for hESC and MSC growth appropriate for cell manufacturing for clinical applications. We demonstrate specification of an MSC-like lineage with a molecular identity and potencies to support haematopoietic progenitor growth and adaptive and innate immune cell modulation distinct from adult human bone marrow (hBM)-MSC and hESC. We propose definition of these or other human pluripotent stem cell derived MSC-like cells as Mesenchymal Stromacytes or simply Stromacytes in recognition of their developmental provenance and distinctiveness.

Methods

Pluripotent Stem Cell Culture

This study utilised the RC-9 hESC line, suitable as seed material for advanced cell therapies, sourced at passage 29 post derivation (De Sousa et al., 2016a, b). All cell culture was performed in 5% CO_2 in humidified air (ie. 20% O_2) at 37 ^{o}C. Cryopreservation of undifferentiated hESC and differentiated derivatives was in Cryostor CS10 (Biolife Solution, Washington, USA). hESC growth and differentiation were in multi-well 6 well tissue culture plates (10cm^2/well; Cellstar, greiner bio-one, Item No. 657960, Stonehouse, UK), or T25 or T75 flasks (VWR, Leighton, Buzzard, UK). Self-renewal of undifferentiated cells was in StemPro™ hESC SFM on planar coatings of CellStart™ substrate (both from Thermofisher, Paisley UK), used according to manufacturer's protocols. Spent/fresh media was exchanged daily 6 days a week. Stock cultures were passaged 1:3 by Easy-Cut cell passaging method at 70–100% confluence (EZPassage, Invitrogen by Life Tech, Paisley, UK).

Differentiation

For differentiation tissue culture plasticware was coated with 0.1mg/ml of hyaluronic acid (HA; 1200 kD, Prod. 385908, Merck-Calbiochem, Nottingham, UK) prepared in Dulbecco's Phosphate Bufferred Saline (DPBS) and filtered with 0.22µm syringe filter. Coating was for at least 1 hour at 4ºC and allowed to reach room temperature before use. Surplus HA solution was aspirated from the wells immediately prior to addition of the cells. HA coating was confirmed by Alcian Blue staining (Corradetti et al., 2017).

For RC-9 differentiation from self-renewal conditions comprised of StemPro™ hESC SFM on CellStart, 100% confluent 6 well plates were dissociated with trypLE Select as per manufacturers protocol to obtain single cells. These cells were then passaged onto HA coated plates at 1:1 for three passages after which they were passaged onto CellStart™ and the media switched to StemPro™ MSC SFM (Life Tech, Paisley, UK).

Other Cell Culture

Adult bone marrow MSC were used as a reference standard procured commercially from Gibco (StemPro™ BM MSC Cat # A15652) and used between passages 3–5 following cultivation in StemPro™

MSC SFM on CellStart™. Cells were cryopreserved in Cryostor CS10 as for hESC.

Haematopoietic Progenitor Growth Assay

Fresh UCB-derived MNC fractions were diluted in Stemline II haematopoietic medium (Sigma Aldrich) containing G-CSF (100ng/ml; Peprotech), SCF (100ng/ml; source), TPO (100ng/ml; source), and Flt 3 ligand (50ng/ml; Life Technologies) and plated over pre-established confluent hESC-MSC in T25 flasks at the following concentrations: 0 (hESC-MP feeder only control), $1x10^4$, $1x10^5$, $2.5x10^5$, $5 x10^5$ and $1x10^6$ MNC per flask. For the MNC-only control MNC were plated at $1x10^6$ MNC per flask in T25 without hESC-MSC. Flasks were incubated and maintained at 37°C, 5% CO_2 in humidified air without media changes. After 7 days of culture, non-adherent cells (ie, MNC fraction containing haematopoietic progenitor/stem cells) were harvested by aspiration of media and subsequent centrifugation at 200 x g for 5 minutes. Pelleted cells were subsequently used for flow cytometric analyses, Total Nuclear Counts (TNC) and Colony Forming Unit (CFU) assays. TNC were determined with the ViaCount® assay on the Guava easyCyte system (Millipore) according to manufacturer's instructions. For the CFU assays, cells were diluted in methylcellulose medium (Methocult, StemCell Technologies) according to manufacturer's instructions using a dissecting microscope and dark field illumination colonies of ≥ 50 cells were characterised and counted. Photographs of Individual colonies were obtained using an Axiocam (Zeiss) and Axiovision software.

Mixed Peripheral Blood Mononuclear Cell Proliferation Assay

The blood mononuclear cell modulatory function of MSCs was assessed in an inhibition of proliferation assay in co-culture with cell tracker dye labelled, mitogen stimulated peripheral blood mono-nuclear cells (PBMNCs). One day prior to addition of PBMNCs doubling dilutions of MSCs were titrated in triplicate in 24 well plate at $2.5x10^5$ cells to $0.3125x10^5$ cells/well in 0.5ml StemMacs medium (SM, Miltenyi Biotec).

PBMNCs were isolated from fresh buffy coats (volume reduced donated units of whole blood obtained from the Scottish National Blood Transfusion Unit) by density gradient separation using Leucosep tubes (Greiner, UK) containing 15ml Ficoll-Paque (GE healthcare, UK). Tubes were centrifuged at 1000 g for 1 minute so that ficoll was below the LeucoSep filter which prevents mixing of blood and Ficoll-Paque. Blood was diluted 1:2 with PBS before 30ml aliquots were pipetted into prepared leucosep tubes and centrifuged at 450g for 40 minutes (acceleration /deceleration at 5). The supernatant volume was reduced to 10ml by pipetting and isolated leucocytes collected by pouring into fresh 50ml tubes, washed once by centrifugation for 7min at 350g. Remaining red blood cells were removed by lysis. The leucocyte pellet was resuspended in 10ml RBC lysis buffer (BioLegend), incubated for 3 minutes at room temperature and topped up with PBS before centrifugation at 350g for 7min. The wash step was repeated and the leucocyte pellet was resuspended in 10ml PBS for counting on a haematology cell counter (Sysmex). 2x108 leucocytes in10ml PBS ($2x10^7$/ml) were labelled with an equal volume of eF450 cell tracker dye at 100nM (Thermofisher) for 20m at 37° C, topped up with TexMACS medium (TM, Miltenyi

Biotec) and incubated at 4°C for 20 minutes. Cells were then washed twice in 50ml TM and resuspended at $1x10^8$/ml in TM.

Labelled PBMC were diluted to $1x10^6$ /ml in TM supplemented 50 IU/ml IL-2 (Peprotech) for addition of 0.5ml to wells with pre-plated MSCs to give final PBMC: MSC ratio of 2:1, 4:1, 8:1, 16:1. Proliferation was stimulated by addition of the mitogen PHA (Sigma) at 5µg/ml Negative control wells omitted PHA and positive control wells containing stimulated PBMNCs alone were included to measure minimum and maximum proliferation respectively. After 6 days culture, at 37°C, 5%CO2 PBMNCs were harvested by aspiration and washing of wells with PBS. After centrifugation for 7m at 350g cell pellets were resuspended in 200µl PBS + 0.5% FCS (Sigma). Halving of fluorescence of labelled daughter cells, in sequential proliferation cycles was measured by flow cytometry using a MacsQuant 10 flow cytometer (Miltenyi Biotec) acquiring 100µl/sample. Data was analysed using FlowJo software (TreeStar). Debris, doublets and dead cells were excluded from analysis based on FSC and SSC characteristics. Inhibition was calculated using in MSC_PBMNC co-cultures relative to% undivided cells in unstimulated negative control.

Immortalised Monocyte Specification Assay

To evaluate potency to modulate innate immune cells, the immortalised monocyte THP1 cell line was obtained from ATCC (https://www.atcc.org/) and maintained at 2 x 10^5 cells/ml in RPMI 1640 medium supplemented with 10% Foetal Calf Serum (FCS) and 2 mmol/L L-glutamine. THP1 cells (2 x 10^5 cells /ml) were differentiated to unspecified macrophages (M) using 100 nM Vitamin D3 (VD3, Sigma-Aldrich) or 200 nM phorbol 12-myristate 13-acetate (PMA, Sigma-Aldrich) for 3d. Differentiation of PMA treated cells was enhanced after the initial 3d stimulus by removing the PMA containing media then incubating the cells in fresh RPMI 1640 (10% FCS, 1% L-glutamine) for a further 5d (PMAr) according to Daigneault et al. (2010).

To assess cell potencies to modulate inflammatory cytokine secretions THP1-M were stimulated with 100 ug/ml Lipopolysaccharide (LPS) concurrently with concurrently con-culture for 24 hours followed by collection and quantification of pro-inflammatory cytokines TNFα and IL6 secretion by Enzyme Linked ImmunoAssays (ELISA) by manufacturers protocols (R&D Systems, Minneapolis, MN, USA). In each experiment co-culture treatments and control LPS treated (ctr LPS+) and untreated in RPMI medium (ctr RPMI) were technically replicated in quadruplicate (n = 4) and normalized with respect to each other in the same assay plate. Inter-plate cytokine assay variation in ctr LPS + levels was 1.5 fold for TNFα (~ 2400–3400 pg/ml) and 3 fold for IL6 (~ 300–900 pg/ml).

Flow Cytometry

Cell phenotype was assessed by flow cytometry using antibodies to CD49a-f, CD29, CD44, CD71, CD73, CD56, CD133, CD13, CD146, CD105, CD90, CD271, CD166, CD34, CD11b, CD45, CD79A, HLA-I and II (Supplementary Table 1). Aliquots of $2x10^5$ cells in 100µl were labelled with optimised concentrations of each antibody separately. After 30min incubation at 4°C samples were washed with 3ml PBS + 0.5% FBS

by centrifugation for 7min. at 350g. Pellets were resuspended in 200 µl PBS + 0.5%FBS for acquisition of data for at least 5,000 events using a MacsQuant10 flow cytometer (Miltenyi Biotec) after exclusion of debris based on FSC and SSC characteristics. Data was analysed using FlowJo software (Treestar). Dead cells and doublet cells were excluded from analysis based on based on FSC and SSC characteristics. Controls (no antibody) were used to set gates for assessment of marker expression.

Phenotyping of UCB-derived MNC was performed according to International Society of Haemotherapy and Graft Engineering (ISHAGE) guidelines (Sutherland et al., 1996). Total UCB and UCB-derived MNC fractions were washed with PBS containing 5% KOSR (Life Technologies), put through a 70µm cell strainer, suspended in the same buffer at $\leq 1x10^6$ cells/ml, and stained in the dark at 5 ± 3°C for at ≥ 15 minutes with the following antibodies: fluorescein isothiocyanate (FITC) conjugated anti-CD45, phycoerythrin (PE) conjugated anti-CD133/2 and allophycocyanin-conjugated anti-CD34 according to the manufacturer's instructions (Miltenyi Biotec). A viability stain, 7-Aminoactinomycin D (7AAD; Cambridge Bioscience), was included to identify live versus dead cells. After staining, cells were washed twice in cold PBS containing 5% KOSR and centrifuged at 500 g for 3 minutes. Cells were acquired and analysed using Guava EasyCyte System (Millipore). For each sample the total number of CD34+, CD133 + and CD34/CD133 double positive cells were calculated within the live (FAAD+) CD45+ (ie, leucocyte) population.

RNAseq

A bulkRNAseq analysis was performed on total RNA concurrently isolated from hESC, hESC derived MSC-like cells and human bone marrow derived (hBM) MSC in the current and adjacent report (De Sousa et al, submitted). To structure the analysis the current study focuses on the subset of samples comprised of the undifferentiated RC9 hESC line in StemPro™ SF medium/CellstartTM matrix @ p35 post derivation; hESC-MSC like cells @ p19 post initiation of differentiation mediated by HA in StemPro™ MSC SFM ; and adult hBM @ p3 in StemPro™ MSC SFM. Each cell type was biologically replicated in quadruplicate samples of $1x10^6$ cryostored cells each.

RNA extractions were carried out using the automated Maxwell RSC Instrument and the Maxwell RSC simplyRNA Cells Kit following the manufacturer's recommendations. RNA concentrations were measured using Qubit RNA High Sensitivity Kit (Invitrogen) and Qubit 4 fluorometer (Invitrogen). RNA integrity was assessed using the 2100 Bioanalyzer (Agilent) with the RNA 6000 Pico kit (Agilent). Library preparation was performed using Illumina the Stranded mRNA kit (Illumina) with TruSeq RNA Single Indexes (Illumina). Preparation was performed as per manufacturer's instructions. cDNA library concentrations were measured using Qubit dsDNA High Sensitivity Kit (Invitrogen) and Qubit 4 fluorometer (Invitrogen). cDNA library quality was checked using 2100 Bioanalyzer (Agilent) with the DNA 1000 kit (Agilent). Libraries were sequenced on the NextSeq 500 platform at 40 bp paired-end reads (41 x 2 cycles) using NextSeq 500/550 High Output Kit v2.3 (75 cycles). Two sequencing runs were performed to achieve the required read count (more than 25 million reads per sample).

Informatics

The standardised RNA sequencing analysis pipeline, nf-core/rnaseq v3.3, was used for quality control, alignment and quantification. Details can be found at https://nf-co.re/rnaseq/3.3. In short, quality control was carried out with FASTQC, adapter and quality trimming with TrimGalore, alignment with STAR and quantification with Salmon. Default settings were used except for STAR “seedSeachStartLmax 25” to increase sensitivity of mapping for 40 bp reads, and TrimGalore “–trim_nextseq 20” to set the Phred score threshold at 20. Reads were aligned to the human genome GRCh37. Count files were imported into R for differential expression analysis with DESeq2 using the default Wald test. P values were adjusted using the Benjamini-Hochberg (BH) method and the threshold for differential expression was BH-adjusted P < 0.05. Gene ontology enrichment and protein-protein interactions analyses were performed using 1) Qlucore Omics Explorer 3.8 (https://qlucore.com/), and ShinyGo 0.77 (Steven et al., 2020). Multi- and two-group comparison of RNA sequence variables were performed at False Discovery Rates (FDR, Q) < 0.05 as reported in figures. Analysis were performed in April 2023. ShinyGO algorithm search parameters of interrogation comprised: Species: Human. FDR cutoff: 0.05; # pathways to show: 20; Pathway size minimum: 2; Pathway size maximum: 2000. Other Options: Redundancies removed, Pathways abbreviated. STRING Pathway Parameters: Human. Display to include up to all genes interrogated.

Statistical Analysis

Non-informatic statistical testing of in vitro culture outcomes was performed using Prism H 5.02 software (GraphPad Software Inc.) by One Way ANNOVA followed by two-tailed post-hoc Dunnett testing of significance.

Results

Hyaluronan mediates derivation of mesenchymal stromal cell-like phenotype in serum-free culture systems

We have previously described the differentiation of an MSC-like lineage utilising Hyaluronan as a planar substrate using the pluripotent H1 and H9 hESC lines (De Sousa, 2012; Velugotla et al., 2012). This was presented in a mouse fibroblast feeder cell conditioned and KOSR supplemented media. We began this study with a pilot assessment to verify this outcome on the RC9 hESC line in a human fibroblast conditioned medium. Over the course of three passages using enzymatic methods of cell dissociation, cultures became enriched with a bi-polar fibroblastic cell morphology which by flow cytometry were positive for common MSC associated markers CD146, CD105 and CD90 (~ 40, 95 and 80%, respectively), and negative for the haematopoietic cell marker CD45 (Suppl. Figure 1). Although the RC9 hESC line was originally derived on mitotically inactivated human fibroblast feeders it was transitioned soon after into cell therapy grade serum- and xeno-free medium (StemPro™ hESC SFM) and matrix (CellStart™) for self-renewal (De Sousa et al., 2016a). We thus next assessed HA substrate mediated differentiation directly from this culture system into a complementary system for serum- and xeno-free MSC culture (Fig. 1. A). Commencing from confluent cultures of the RC9 hESC line under self-renewal conditions, three successive passages of enzymatic dissociation and plating of single cells also yielded a comparable

progressive loss of undifferentiated cell colonies and enrichment of a bipolar fibroblastic morphology (Fig. 1B). As with the original method we observed proliferation of these cells in excess of 20 passages in a serum- and xeno-free media designed for cultivation of MSC before retardation of growth became evident practically (data not shown).

To characterise hESC-MSC-like cells, here forth referred to as human Mesenchymal Stromacytes (hMS) or simply Stromacytes, differentiated by virtue of cultivation on a planar substrate of HA in serum and xeno-free culture, we focused on late passage (p) 19 post initiation of differentiation. Independent batches of these were expanded from a cryostored working bank of cells at p15/16 post HA. We first assessed expression of cell surface markers of MSC identity by flow cytometry on two independently generated batches of cells from this working bank. Batches were broadly consistent in forward and side scatter (FSC, SSC) which reflected a greater range in cell diameter and volume (FSC) than cell complexity (SSC) that was low (Suppl. Figure 2), Cells expressed a range of markers commonly associated with adult tissue derived MSC from various sources (eg. Bone, adipose, placental). In descending order of abundance and consistency between batches these were: CD44, CD13, and HLA-I (> 95%); CD166, CD90 and CD73 (70–100%); CD56 (30–40%); and CD105 (15–75%). Cells were predominantly negative for other adult tissue derived MSC-associated markers, namely CD71 and CD271 (~ 5–10%) and CD146 (~ 1–10%). They were also negative for markers not associated with MSC, namely HLA-II and other haematopoietic progenitor lineage markers such as CD34, CD45, CD14 and CD133. Assessment of integrin subunit expression revealed in descending order of abundance and consistency between batches: Integrin alpha 2 & 5 (~ 70–100%); 3 (50–90%); 1, 6 and beta 1 (~ 25–65%) (Fig. 1C, Suppl. Figures 3 & 4). On the basis of markers assessed, hMS identify as MSC according to ISCT minimal essential criterion of expression of CD73, 105 and 90 and absence of CD34, CD45 and CD14, the latter denoting an absence of haematopoietic lineages. Expression/absence of other MSC associated markers and integrin subunit profiles flag the likely distinctiveness from primary tissue derived sources and cell-extracellular matrix interaction potential.

Mesenchymal Stromacytes present MSC-like functional properties in co-culture

MSC are valued for their potency to mediate tissue repair through cell-cell contact and soluble paracrine effects on haematopoietic and tissue resident cells (Bianco et al., 2019). We thus next investigated functional potencies of hMS to support growth and modulate behaviour of haematopoietic lineages in co-culture. We first considered their capacity to support in vitro expansion of umbilical cord blood derived haematopoietic progenitors, namely CD34 and CD133 double positive mononuclear cells as has been shown for human bone marrow (hBM) derived MSC (Robinson et al., 2011). Specifically we evaluated yield of these after seven days of co-culture with three independently replicated batches of hMS at p19 post HA differentiation. Each of these was cultured with 3 escalating doses of independent batches of Umbilical Cord Blood-Peripheral Blood Mononuclear Cells (UCB-PBMC)(Suppl. Figure 5A). UCB PBMC co-cultured with hMS consistently yielded more CD34/CD133 + cells than in the absence hMS. These retained differentiation potential to form Burst Forming Units of erythroid colonies (BFU-E), and

progression to late-stage colony units of granulocyte-macrophage progenitors (CFU-GM) and granulocyte, erythrocyte, monocyte, and megakaryocytes (CFU-GEEM) (Shown for co-culture Fig. 2B). Merger of differentiated colonies precluded quantification of differentiated progenitor yields. In 2/3 of experiments, yield was directly proportional to UCB PBMC starting number (Fig. 2A, B).

To investigate hMS ability to modulate immune cell responses we assessed capacity to inhibit mitogen activated proliferation of peripheral blood mononuclear cells (PBMC) in co-culture (Rasmusson et al 2005; Suppl. Figure 5). In the absence of hMS, addition of PHA increased the proportion of maximally proliferated cells from approximately 10% (without PHA treatment) to 70%. This increase in proliferation was reduced when PBMC were co-cultured in the presence of hMS with stronger effects observed at the higher hMS ratios confirming hMS aability to inhibit PBMC proliferation (Fig. 2C representative outcome).

Finally to investigate hMS co-culture ability to modulate innate immune cell responses we used an immortalised THP1 monocyte as a source of macrophages (M) (Daigneault et al, 2010) from which pro- to anti-inflammatory subtypes (ie. M1/M2 variants, respectively) can be specified following stimulation with an inflammatory stimulus (lipopolysaccharide, LPS, concurrent with modulating treatments. In this assay, we quantified levels of inflammatory cytokines TNFα and IL6 in culture medium 24 hr after LPS stimulation +/- hMS co-culture, these cytokines serving as a surrogate measure of inflammatory status (Suppl. Figure 5c). Three independent batches of hMS @p19 post HA differentiation were evaluated at hMS:THP1 M ratios of 1:4 and 1:8 with THP1. In the absence of cell co-culture, LPS treatment increased soluble TNFα and IL6 levels over 10 fold. As compared with LPS treatment alone, hMS co-culture had no (2 batches) or a minor (1 batch) significant reduction in TNFα at both cell co-culture ratios. In contrast, co-culture significantly increased IL-6 levels at both ratios for all 3 batches (Fig. 3). A comparable outcome was first reported for the capacity of hBM-MSC to modulate an M2 subtype from peripheral blood derived monocytes in the absence of pretreatments to licence hBM-MSC immunomodulatory potency (Kim and Hematti, 2009). Thus, hMS have a potential to modulate primary macrophage specification.

RNA phenotyping of Stromacyte identity

Given the similarities between hMS and hBM-MSC in morphology (Fig. 4A), surface marker expression and potencies to modulate haematopoietic lineages we next compared these and source hESC samples by bulk RNAseq. In excess of 196,000 RNA sequence variables associated with a total of 20,964 genes were assessed. Paired comparisons of total gene expression of hMS with both hESC and hBM-MSC manifest comparable ranges of fold changes although there was less difference and significance in the latter comparison (Suppl. Figure 6). Similarity with hBM-MSC and greater distance from hESC was further reinforced by principle component analysis and heat map profiling of the top 500 differentially expressed transcripts (Fig. 4B & C).

We first examined the expression of a selection of 45 genes associated with MSC potency to support haematopoietic progenitor expansion (Pineault and Abu-Khader, 2015), adaptive immune T-cell suppression (Haddad et Saldanha-Araujo, 2014), and innate immune macrophage specification (Lu et al., 2021). Genes were selected from BulkRNAseq data on the basis of one or more ENSEMBL ID transcripts

associated with a gene being detected in all biological replicates of at least one of the three sample cell types. Transcript expression is presented as Average Number of Transcripts per Million for Gene Symbols to which Ensembl ID relate. Most genes were expressed in all 3 cell types and expression in hMS was comparable or greater to that in hBM-MSC (Fig. 5). Of 6 selected genes associated with support of haematopoietic progenitor expansion (KTLG, FLT3LG, ANGPTL4, ANGPTL2, ANGPT1 and IGFBP2), IGFBP2 expression was the most prominently expressed and in hESC and hMS versus hBM-MSC, respectively (Fig. 5A). Of 22 selected genes involved in MSC suppression of T-cells by indirect soluble proteins (LIF, HMOX1), soluble PGE2 (PTGS1, PTGES3, PTGES2, PLA2G12A, LYPLA2), direct soluble proteins (TGFB1, SEMA3A, LGALS1), cell contact (ITGB1, ITGAV, ITGA6, ITGA5, ITGA3) and TNF licencing (TNFRSF1A, MAPK3, MAPK1, AKT3, AKT2, AKT1, AK1), LGALS1 and ITGB1 were the most prominently expressed and equally so in hMS and hBM-MSC (Fig. 5b). And of genes involved in macrophage specification via soluble paracrine factors (CCL2, CXCL12, VEGFC, B, A, TNFAIP6, TGFB1, PTX3, IGFBP3, CSF1), miR (MIR24-2) and ECM and membrane interactions (COL6A3, COL6A1, IL1R1, ICAM1, aCD200), COL6A3 and 1 were the most prominently expressed and greatest in hMS (Fig. 5C).

We then carried out gene set enrichment for an unbiased assessment of differences between hMS, hESC and hBM-MSC .We focused on paired comparisons of Gene Ontologies (GO) terms for Biological Process and Curated Reactomes available in the ShinyGO 0.77 platform, the latter chosen to augment understanding of cell differentiation potency and functionality. For each we assessed the top 20 GO terms that were significantly enriched by all genes upregulated and downregulated by more than 2-fold (Suppl. Figures 7–10) and subsets of genes upregulated by more than a hundred fold (Fig. 6, 7 and Suppl. Figure 11–12).

Querying all 4,246 transcripts upregulated ≥ 2-fold in hMS compared with hESC the top 20 Biological Process GO terms manifest as four clusters centred on cell motility and adhesion; vascular development and tissue morphogenesis; skeletal system development; and extracellular matrix organisation. GO terms within these clusters were enriched 2–3 fold by 100's of genes in each (Suppl. Figure 7A. 8A; FDR ≤ -$\log_{10}$45). When considering the top 25 RNA transcripts upregulated by 2000-fold or greater, significantly enriched GO terms were essentially the same, now associated in 3 clusters. Each component GO term was enriched in excess of 10 fold by 5–10 genes each (Fig. 6; FDR –$\log_{10}$4). The top 20 Curated Reactomes for all transcripts upregulated ≥ 2 comprised twelve GO term clusters encompassing interactions, biosynthesis, transport, and signalling of syndecan, collagen, IGF, Receptor Tyrosine Kinase and Interleukins, respectively; cell-ECM interactions; vesicle transport; post-translational protein modification; smooth muscle contraction, blood hemostasis via platelet activation signalling and aggregation; cytokine signalling in the immune system; and neutrophil degradation (Suppl. Figure 11; FDR ≤-$\log_{10}$8). By contrast, querying all 5715 transcripts downregulated ≥ 2-fold in hMS vs hESC the top 20 GO terms for Biological Process was comprised of seven clusters each enriched 1–3 fold by 100's of genes centred on DNA replication; recombinatorial repair; neurogenesis; ion cation transport; regulation of membrane potential; trans-synaptic signalling; and circulatory system processes (Suppl. Figure 7B, 8B; FDR ≤ -$\log_{10}$10). Collectively these may indicate cell acquisition of a mesendodermal phenotype at the

expense of undifferentiated processes and ectodermal lineage fate. To identify potential master regulators of hMS identity we interrogated the STRING database (von Mering et al., 2005) for known and predicted protein interactions, for proteins encoded by the top 25 upregulated genes, an arbitrary threshold at which the log fold change in individual genes ranged from 2^{11-17}. This predicted 88 interactions substantially exceeding 15 expected randomly. The nexus of this interaction network is Paired Related Homeobox 1 (PRRX1) interacting with other homeobox genes (HOXB3, 4, 5), a transcription factor of an orphan nuclear receptor (NR2F2) and collagen subunits (notably COL3A1) (Suppl. Figure 13, p = 0). This nexus suggests a specific developmental and anatomical positioning of cell identity and function for which Collagen is an upstream driver when compared with undifferentiated cells.

Stromacyte gene expression supports an earlier developmental phenotype when compared to bone marrow MSC

Whereas when compared with hESC, hMS transcriptome reflects a shift away from ectoderm lineage, comparison with hBM-MSC suggests that this progression is incomplete. Querying the 2090 transcripts upregulated ≥ 2-fold in hMS when compared with hBM-MSC hBM-MSC, the top 20 Biological Process GO terms manifest as four clusters centred on cell adhesion; migration, junction organisation; and projection morphogenesis and neuron formation. GO terms within each of these clusters were enriched 2–5 fold by 100's of genes (Suppl. Figure 9A. 10A; FDR ≤ $-\log_{10}24$). A narrowed consideration of GO terms for the top 25 and 50 upregulated genes upregulated by 2^{8-9} fold yielded a single cluster centred on Regulation of Cellular Response to Growth Factor Stimulus, namely to BMP, Phospholipase C and Neurotrophin-Tyrosine Receptor Kinase receptor signalling pathways and urogenital morphogenesis (Shown for top 50, Fig. 7, 2–8 genes per GO, FDR < 0.03). The top 20 curated Reactomes for all transcripts upregulated ≥ 2 fold comprised nine GO term clusters encompassing GPCR ligand binding; NCAM interactions; axon guidance; Tyrosine Receptor Kinase signalling; EPH-ephrin mediated cell repulsion; Neuronal system; muscle contraction; and Collagen fibril assembly (Suppl. Figure 12, FDR ≤ -log105). By contrast, the top 20 Biological Process GO terms querying all 2090 transcripts downregulated ≥ 2-fold in hMS vs hBM-MSC comprised eight clusters each enriched approximately 2–3 fold with 40–160 associated genes centred on ossification; cell adhesion; homeostasis; circulatory system processes; urogenital system development; regionalisation; skeletal development; and circulatory system development (Suppl. Figure 9B, 10B, FDR ≤ -log106). Collectively, these results support interpretation of an earlier developmental phenotype for hMS when compared with hBM-MSC. Lastly, to further clarify prospective master regulators of hMS identity and potency we interrogated the STRING database for known and predicted protein interactions with proteins encoded by top 50 upregulated transcripts relative to hBM-MSC. This predicted 37 proteins to have 99 interactions exceeding 40 expected randomly. The nexus of this network is Bone Morphogenic Protein 7, connecting to other hubs centred on Neurotrophic Receptor Tyrosine Kinase 3 (NTRK3) and LIM homeobox 8 (LHX8) (Suppl. Figure 14, p = 3.11e-15). These pertain to

processes of tissue and cell morphogenesis and differentiation consistent with an earlier developmental phenotype.

Discussion

Here we report the differentiation of a proliferative MSC-like cell population from pluripotent human embryo stem cells, by virtue of growth on a planar coating of HA in serum-free media systems. In vitro these cells have haematopoietic progenitor expansion supportive and adaptive and innate immune cell modulating potencies commonly attributed to adult tissue derived MSCs, and a similar molecular identity by cell surface marker flow cytometry and bulk RNAseq. Despite the observed similarities the latter sequencing analysis suggests that cells produced by the method described in this paper are clearly more developmental in their identity. They are thus likely to offer greater tissue generative potencies than adult tissue derived MSC in addition to blood lineage modulating capacity necessary to tissue repair. The need for more precise nomenclature to recognise the more developmental phenotype associated with pluripotent stem cell vs adult tissue has been previously cited (West et al., 2016). In acknowledgement we have favoured discrimination of developing mesenchymal stromal cells as stromacytes.

In the last twenty years, an MSC-like identity and functionality has been differentiated from human pluripotent stem cells by different approaches, all of which have reached a similar conclusion of producing a more developmental phenotype (reviewed in Jiang et al., 2019). The first comprised culture based methods, including: 1) co-culture with a murine (OP9) feeder cell (Barberi et al., 2005); 2) embryoid body mediated differentiation (Mahmood et al., 2010); and 3) spontaneous differentiation of adherent cells in cell feeder-free but conditioned culture. All of these methods included supplementation of culture with blood serum (Lian et al., 2006; Trevidi and Hematti, 2008; Karlsson et al., 2009; Boyd et al., 2009; Olivier et al., 2006). A next generation of methods have applied small molecules to manipulate developmental signal transduction events at the heart of mesendoderm vs ectoderm specification (eg. Sanchez et al., 2011; Zhao et al., 2015). Specifically, by virtue of modulating the strength, duration and combination of suppression of BMP and TGFβ signal mediators coupled with activation of WNT, it is now possible to differentiate and regionalise presomatic mesoderm, nascent and developed somites and subsequent dermomyotome and sclertome from hPSC (Xi et al., 2017). This has offered greater control in the in vitro specification of mesoderm and tissue specific mesenchymal stromal cells. Prior understanding of HA's role as both instigator and modifier of tissue morphogenesis and cell specification inspired both our and other group explorations of its potential to control pluripotent stem cell behaviour and fate. Like small molecule based methods, our differentiation in serum-free media systems further affirms that differentiation can be achieved without recourse to the complexity of factors serum provides. The proprietary and undisclosed composition of the media used in our study precludes further understanding and dissection of the role and interaction of HA with other cognate factors in the media. However, our results substantiate HA as a determinant of MSC-like fate from pluripotent stem cells.

Planar (2D) cell-adherent culture of human pluripotent stem cells commonly requires either a substrate coating of integrin binding proteins (eg. fibronectin, laminin, vitronectin) or synthetic surfaces which can

mimic what these provide through polymer chemistry and topography (Lambshead et al., 2013). We observed a high degree of non-adherent cell loss in passaging confluent cultures of hESC to HA. This was also seen in the absence of any coating although in this case cells which did adhere failed to proliferate. Thus, although one aspect of our approach may involve subculture of hPSC or differentiating derivatives capable of adhering to polystyrene plasticware surfaces (as well as to a HA substrate coating if provided), HA is essential for promotion of subsequent growth of these cells. In an adjacent study to this one we have further investigated the mechanism of HA actions in molecular defined media and matrix. This has provided cell transcriptome, cell secretome proteome and inflammatory cytokine modulation assay evidence that HA primes differentiation of hESC and functional maturation of stromacytes differentiated there from (De Sousa et al., in preparation).

At the level of CD surface markers associated with adult tissue derived MSC identity, stromacytes produced in this study lacked CD271 (p75 Low Affinity Nerve Growth Factor Receptor), CD71 (Transferrin Receptor) and CD146 (Melanoma Cell Adhesion Molecule MCAM). CD271 is regarded as an unsuitable universal MSC marker before culture of cells from tissue sources and is inadequate for isolation of MSC from developmental tissues such as umbilical cord blood and Whorton's jelly (Alvarez-Viejo et al., 2014). However expression of this surface marker in adipose MSC is associated with higher expression of angiogenic genes and neoangiogenic potential (Smith et al., 2021). CD71 is an MSC marker associated with cell proliferation. Its absence is consistent with our assessment of late passage cells (Moracikova et al., 2018). CD146 expression on MSC is associated with their vascular smooth muscle commitment (Espagnolle et al., 2014).

Observed stromacyte potency to support and modulate haematopoietic cell lineages was accounted for by assessment of a selection of associated genes. Notable amongst these were IGFBP2; Galectin-1 and Integrin Beta 1; and Collagen VI subunits A3 and A1 with respect to haematopoietic progenitor expansion, suppression of lympohycte proliferation and macrophage specification, respectively. IGFBP2 supports the survival and cycling of hematopoietic stem cells (Huynh et al., 2011). Galectins are a class of 15 cell surface and secreted proteins which bind to β-galactoside sugars, such as N-acetyllactosamine. Several members including Galactin-1 have been implicated in tissue MSC potency to modulate adaptive and innate immune cells. (Gieseke et al., 2010). Integrin B1 is required for MSC survival and directed migration on collagen and fibronectin substrates in tissue repair (Ip et al., 2007; Zwolanek et al., 2015). Collagen 6 forms as a unique microfibrillar network between the basement membrane and interstitial matrix of cells and tissues. Congenital mutations in subunits (COL6A1, A2 and A3) cause Ulrich muscular deficiency, a skeletal muscle regeneration deficiency wherein muscle stromal cells support skeletal muscle satellite stem cell renewal and homeostasis through several secreted factors including Collagen VI (Takenaka-Ninagawa et al., 2021). Collagen VI has been shown to modulate macrophage activation and cellular functions and other innate and adaptive immune cells directly and indirectly during tissue repair (Sapudom et al., 2020). The cleaved C5 domain of collagen VI alpha 3 chain is a pan-cancer biomarker of poor prognosis and resistance to chemotherapy implicated in tumorigenesis by various mechanisms including sustaining cell stemness; promotion of epithelial to mesenchymal transition, cell migration and angiogenesis (Wang and Pan, 2020).

Top stromacyte enriched GO terms compared to both hESC and hBM-MSC included cell motility and adhesion consistent with HA associated biological processes and a developmental phenotype. Depending on the comparator this was associated with tissue morphogenesis, notably vascular, urogenital and skeletal (wrt hESC) and cell projection and synapse formation (wrt hBM-MSC). Comparison with the latter reflected a multitude of cellular responses to growth factor stimulus, namely to BMP, Phospholipase C and Neurotrophin-Tyrosine Receptor Kinase receptor signalling. Top differentially expressed genes in either comparison featured HOX (HOXB3, 4, 5 and associated major transcriptional regulators (PRRX1, LIM homeobox18, NR2F2) interacting and likely regulating downstream expression of collagen subunits (COL3A1), BMP7 and Neurotrophic Receptor Tyrosine Kinases (NTRK3). Despite the uniformity of morphology in culture hMSC, cell heterogeneity is likely to have existed which our utilisation of bulk RNA sequencing would not discriminate. Thus, the extent to which these molecules interplay within each other within any given cell is unclear. However, understanding the prominence of expression of these molecules provides the foundation to future work to understand and manipulate cell identity and potencies to differentiate or modulate other cells. For example, homeobox genes specify regions of the body plan of an embryo along the head-tail axis and determine cell fate and tissue patterning during tissue morphogenesis. In mammalian development HOXB3 is expressed in hindbrain rhombomeres that regulate the development of hindbrain cranial and motor neurons. It is also expressed along with HOXB4, and B5 as well as other HOX paralogs along the anterior to posterior axis in developing thymus and lung tissue and proximate skeletal vertebrae (Hubert et al., 2023). BMP7 promotes both chondrogenic and osteogenic differentiation in MSC (Shen et al., 2010) and its transgenic overexpression in hBM-MSC improves effectiveness in healing bone fractures as compared with non-transgene expressing cells (Yan et al., 2018).

Conclusions

In conclusion we report here that cultivation of human pluripotent stem cells on a planar substrate of HA in serum-free culture media systems is sufficient to yield a distinctive developmental mesenchymal stromal cell lineage we term stromacytes. The utilisation of serum-free culture systems, simplicity of the method, and the proliferative capacity of resulting cell populations all favour future scaling of cell manufacture for therapeutic applications. In vitro assessments of functional potency and molecular assessment of identity by flow cytometry and RNA sequencing substantiate prospective therapeutic utilities for both tissue repair and generation.

Abbreviations

HA Hyaluronan

hESC human Embyro Stem Cells

hBM human Bone Marrow

MSC Mesenchymal Stromal Cells

hMS Mesenchymal Stromacytes (Stromacytes)

Declarations

Ethics approval and consent to participate

The hESC line used in this study (RC9) was derived in the project entitled *Human Embryo Stem Cell Derivation for Clinical applications*. The project was approved by Scotland A Research Ethics Committee (Reference 07/MRE00/56, 31 July 2006). Research was conducted under licence from the UK Human Fertilisation and Embryology Authority (No. R0136). The processing and storage of hESC for human application was conducted under licence number 22631 from the UK Human Tissue Authority (De Sousa et al., 2016 a,b).

Fresh full-term cord blood fractions were obtained from patients at Edinburgh Royal Infirmary, Obstetrics and Gynaecology department. The project was entitled *Examination of the potential of human tissue (adult) stem and progenitor cells for regenerative therapies (IRAS Project ID: 12361)*. This was approved by The South East Scotland Research Ethics Committee 2 (Reference 09/S1102/35, 30 September 2010).

Consent for publication

Not applicable.

Availability of data and materials

The RC9 (RCe013-A) cell line was derived in compliance with EU Tissues and Cells Directives and UK Human Fertilisation and Embryology and Human Tissue Authority licenses warranting ethical procurement and utility to serve as source material for advanced therapies in the EU. It is registered with the EU hPSC$^{reg®}$ (https://hpscreg.eu/cell-line/RCe013-A) and can be procured for evaluation and as source material for product development from the UK National Institute for Biological Standards (NIBSC) UK Stem Cell Bank (UKSB) (https://www.nibsc.org/ukstemcellbank).

The raw datasets generated andr analysed during the current study are not publicly available due to commercial sensitivity. Differentially expressed gene lists are available for non-commercial use from the corresponding author under confidentiality agreement on reasonable request.

Competing interests

PDS and AC are co-founders and persons with controlling interests in Stroma Therapeutics Ltd. EA is currently an employee of AstraZenica. All other authors declare that they have no competing interests.

Funding

This research was supported by grants from the former UK Technology Strategy Board to PDS and AC and UK Research & Innovation Innovate UK to PDS, AC, TMW and DD (Project Ref. 85447).

Authors' contributions

PDS led the design and management of studies, RNAseq analysis, interpretation of experiments and manuscript drafting. EA, TMW, DD and AC contributed to project leadership. JY led in the development of cell differentiation method and umbilical cord blood MNC co-culture experiments. KS led in the performance and analysis of flow cytometry and PBMC MLR studies. MG and RM performed RNA isolation and RNAseq and LP performed primary analyses. EP executed and analysed THP1 co-culture experiments designed by DD. PDS and AC secured grant funding for studies. All authors read and approved the final manuscript."

Acknowledgements

EP was financed by the Polish National Agency for Academic Exchange (NAWA) within Bekker Program. TMW is supported by ISP funding from the BBSRC (3 BBS/E/RL/230001C 2023-present and BBS/E/D/10002071 2017-23.The authors would like to thank Dr John Campbell and Prof Marc Turner for helpful advice at the onset of this study, and Ms Kelly McDonald, Mr Gregor Russell, and Dr James Alibhai for technical contributions and Mr Kevin Bruce, Dr Marieke Hoeve for contributions to team management of research. No work was outsourced.

Authors' information

PDS has over 25 years’ experience leading life sciences discovery, innovation and commercial translation in reproductive and stem cell & regenerative medicine biotechnology for disease modelling, screening, and therapeutic applications (ORCID ID 0000-0003-0745-2504).

LP is a principal scientist at the MHRA with a background in neuroscience and stem cell biology. Work. His work focuses on supporting the development of safe and effective cell therapies.

JY has over 25 years’ research experience in embryo biotechnology and stem cell biology, focusing on stem cell derivation, differentiation, and commercial translation, in multiple universities and biotech companies of both the UK and China (ORCID ID 0000-0002-1441-6950).

KS has over 30 years research experience in human and animal modelling of haematopoietic stem cell lineage isolation, culture and expansion.

EP is an assistant professor in the Department of Molecular Biology at the University of Gdańsk, her research interest is in understanding molecular mechanisms of metabolic and autoimmune disorders (ORCID ID 0000-0002-8899-2010).

EA has over 20 years of experience in the pluripotent stem cell field, ranging from applied research through to manufacturing and regulatory compliance of stem cell-derived products (ORCID ID = 0000-

0003-4493-6065).

TMW is Prof of Molecular Anatomy with expertise in model systems and -omics. (ORCID ID 0000-0002-1973-6654).

DHD is Prof of Infection Medicine and clinician scientist specialising in macrophages in host defence against bacteria and viruses with emphasis on microbicide mechanisms and cell death paradigms in pulmonary infection and human immunodeficiency virus (HIV).

AC has over 25 years' experience building life sciences companies.

References

1. Álvarez-Viejo M, Menéndez-Menéndez Y, Otero-Hernández J. CD271 as a marker to identify mesenchymal stem cells from diverse sources before culture. World J Stem Cells. 2015 Mar 26;7(2):470-6. doi: 10.4252/wjsc.v7.i2.470. PMID: 25815130; PMCID: PMC4369502.
2. Amann E, Wolff P, Breel E, van Griensven M, Balmayor ER. Hyaluronic acid facilitates chondrogenesis and matrix deposition of human adipose derived mesenchymal stem cells and human chondrocytes co-cultures. Acta Biomater. 2017 Apr 1;52:130-144. doi: 10.1016/j.actbio.2017.01.064. Epub 2017 Jan 25. PMID: 28131943.
3. Barberi T, Willis LM, Socci ND, Studer L. Derivation of multipotent mesenchymal precursors from human embryonic stem cells. PLoS Med. 2005 Jun;2(6):e161. doi: 10.1371/journal.pmed.0020161. Epub 2005 Jun 28. PMID: 15971941; PMCID: PMC1160574.
4. Bianco P, Gehron-Robey P, Simmons PJ. Mesenchymal Stem Cells: Revisiting history, concepts and assays. Cell Stem Cell 2008, Vol 2, No. 4, Pages 313-319, ISSN 1934-5909, https://doi.org/10.1016/j.stem.2008.03.002.
5. Bonafè F, Govoni M, Giordano E, Caldarera CM, Guarnieri C, Muscari C. Hyaluronan and cardiac regeneration. J Biomed Sci. 2014 Oct 30;21:100. doi: 10.1186/s12929-014-0100-4. PMID: 25358954; PMCID: PMC4226915.
6. Boyd NL, Robbins KR, Dhara SK, West FD, Stice SL. Human embryonic stem cell-derived mesoderm-like epithelium transitions to mesenchymal progenitor cells. Tissue Eng Part A. 2009 Aug;15(8):1897-907. doi: 10.1089/ten.tea.2008.0351. PMID: 19196144; PMCID: PMC2792108.
7. Brown JJ, Papaioannou VE. Ontogeny of hyaluronan secretion during early mouse development. Development 1993 117, 483–492.
8. Cowman MK, Lee HG, Schwertfeger KL, McCarthy JB, Turley EA. The Content and Size of Hyaluronan in Biological Fluids and Tissues. Front Immunol. 2015 Jun 2;6:261. doi: 10.3389/fimmu.2015.00261. PMID: 26082778; PMCID: PMC4451640.
9. Corradetti, B., Taraballi, F., Martinez, J.O. et al. Hyaluronic acid coatings as a simple and efficient approach to improve MSC homing toward the site of inflammation. Sci Rep 7, 7991 (2017). https://doi.org/10.1038/s41598-017-08687-3

10. Cui X, Huang C, Chen Z, Zhang M, Liu C, Su K, Wang J, Li L, Wang R, Li B, Chen D, Ruan C, Wang D, Lu WW, Pan H. Hyaluronic acid facilitates bone repair effects of calcium phosphate cement by accelerating osteogenic expression. Bioact Mater. 2021 Apr 8;6(11):3801-3811. doi: 10.1016/j.bioactmat.2021.03.028. PMID: 33937587; PMCID: PMC8058907.
11. Daigneault M, Preston JA, Marriott HM, Whyte MKB, Dockrell DH. The Identification of Markers of Macrophage Differentiation in PMA-Stimulated THP-1 Cells and Monocyte-Derived Macrophages. PLoS ONE 2010, 5(1): e8668. https://doi.org/10.1371/journal.pone.0008668
12. De Sousa PA. Culture of mammalian pluripotent stem cells in the presence of hyaluronan induces differentiation into multi-lineage progenitor cells. United States Patent No. US 8,110,400 B2. Feb 7, 2012.
13. De Sousa PA, Tye BJ, Bruce K, Dand P, Russell G, Collins DM, Greenshields A, McDonald K, Bradburn H, Canham MA, Kunath T, Downie JM, Bateman M, Courtney A. Derivation of the clinical grade human embryonic stem cell line RCe013-A (RC-9). Stem Cell Res. 2016a Jul;17(1):36-41. doi: 10.1016/j.scr.2016.04.020. Epub 2016 May 6. PMID: 27558601.
14. De Sousa PA, Downie JM, Tye BJ, Bruce K, Dand P, Dhanjal S, Serhal P, Harper J, Turner M, Bateman M. Development and production of good manufacturing practice grade human embryonic stem cell lines as source material for clinical application. Stem Cell Res. 2016b Sep;17(2):379-390. doi: 10.1016/j.scr.2016.08.011. Epub 2016 Aug 26. PMID: 27639108.
15. De Sousa PA, Ritchie D, Green A, Chandran S, Knight R, Head MW. Renewed assessment of the risk of emergent advanced cell therapies to transmit neuroproteinopathies. Acta Neuropathol. 2019 Mar;137(3):363-377. doi: 10.1007/s00401-018-1941-9. Epub 2018 Nov 27. PMID: 30483944; PMCID: PMC6514076.
16. De Sousa PA, Piotrowska E, Sarah H, Mee J, Perfect L, Kurian DT, Abranches E, Mearns-Spragg A, Wishart TM, Dockrell D, Courtney A. Hyaluronan in mesenchymal cell lineage differentiation from human embryo stem cells: Part 2, Priming lineage specification & maturation. Stem Cell Research & Therapy (Submitted)
17. Espagnolle N, Guilloton F, Deschaseaux F, Gadelorge M, Sensébé L, Bourin P. CD146 expression on mesenchymal stem cells is associated with their vascular smooth muscle commitment. J Cell Mol Med. 2014 Jan;18(1):104-14. doi: 10.1111/jcmm.12168. Epub 2013 Nov 4. PMID: 24188055; PMCID: PMC3916122.
18. Fletcher JM, Ferrier PM, Gardner JO, Harkness L, Dhanjal S, Serhal P, Harper J, Delhanty J, Brownstein DG, Prasad YR, Lebkowski J, Mandalam R, Wilmut I, De Sousa PA. Variations in humanized and defined culture conditions supporting derivation of new human embryonic stem cell lines. Cloning Stem Cells. 2006 Winter;8(4):319-34. doi: 10.1089/clo.2006.8.319. PMID: 17196096.
19. Gerecht S, Burdick JA, Ferreira LS, Townsend SA, Langer R, Vunjak-Novakovic G. Hyaluronic acid hydrogel for controlled self-renewal and differentiation of human embryonic stem cells. Proc Natl Acad Sci U S A. 2007 Jul 3;104(27):11298-303. doi: 10.1073/pnas.0703723104. Epub 2007 Jun 20. PMID: 17581871; PMCID: PMC2040893.

20. Gieseke F, Böhringer J, Bussolari R, Dominici M, Handgretinger R, Müller I. Human multipotent mesenchymal stromal cells use galectin-1 to inhibit immune effector cells. Blood. 2010 Nov 11;116(19):3770-9. doi: 10.1182/blood-2010-02-270777. Epub 2010 Jul 19. PMID: 20644118.
21. Haddad R and Saldanha-Araujo F. Mechanisms of T-cell immunosuppression by mesenchymal stromal cells: What do we know so far? 2014, Article ID 216806. doi.org/10.1155/2014/216806,
22. Harkness L, Mahmood A, Ditzel N, Abdallah BM, Nygaard JV, Kassem M. Selective isolation and differentiation of a stromal population of human embryonic stem cells with osteogenic potential. Bone. 2011 Feb;48(2):231-41. doi: 10.1016/j.bone.2010.09.023. Epub 2010 Sep 30. PMID: 20869473.
23. Hubert KA, Wellik DM. Hox genes in development and beyond. Development 1 January 2023; 150 (1): dev192476. doi: https://doi.org/10.1242/dev.192476
24. Huynh H, Zheng J, Umikawa M, Zhang C, Silvany R, Iizuka S, Holzenberger M, Zhang W, Zhang CC; IGF binding protein 2 supports the survival and cycling of hematopoietic stem cells. Blood 2011; 118 (12): 3236–3243. doi: https://doi.org/10.1182/blood-2011-01-331876
25. Ip JE, Wu Y, Huang J, Zhang L, Pratt RE, Dzau VJ. Mesenchymal Stem Cells Use Integrin β1 Not CXC Chemokine Receptor 4 for Myocardial Migration and Engraftment. Molecular Biology of the Cell 2007 18:8, 2873-2882
26. Jiang B, Yan L, Wang X, Li E, Murphy K, Vaccaro K, Li Y, Xu RH. Concise Review: Mesenchymal Stem Cells Derived from Human Pluripotent Cells, an Unlimited and Quality-Controllable Source for Therapeutic Applications. Stem Cells. 2019 May;37(5):572-581. doi: 10.1002/stem.2964. Epub 2019 Jan 21. PMID: 30561809.
27. Karlsson C, Emanuelsson K, Wessberg F, Kajic K, Axell MZ, Eriksson PS, Lindahl A, Hyllner J, Strehl R. Human embryonic stem cell-derived mesenchymal progenitors–potential in regenerative medicine. Stem Cell Res. 2009 Jul;3(1):39-50. doi: 10.1016/j.scr.2009.05.002. Epub 2009 May 19. PMID: 19515621.
28. Kim J, Hematti P. Mesenchymal stem cell-educated macrophages: a novel type of alternatively activated macrophages. Exp Hematol. 2009 Dec;37(12):1445-53. doi: 10.1016/j.exphem.2009.09.004. Epub 2009 Sep 20. PMID: 19772890; PMCID: PMC2783735.
29. Kim IL, Mauck RL, Burdick JA. Hydrogel design for cartilage tissue engineering: a case study with hyaluronic acid. Biomaterials. 2011 Dec;32(34):8771-82. doi: 10.1016/j.biomaterials.2011.08.073. Epub 2011 Sep 7. PMID: 21903262; PMCID: PMC3183132.
30. Kim SN, Lee HJ, Jeon MS, Yi T, Song SU. Galectin-9 is Involved in Immunosuppression Mediated by Human Bone Marrow-derived Clonal Mesenchymal Stem Cells. Immune Netw. 2015 Oct;15(5):241-51. doi: 10.4110/in.2015.15.5.241. Epub 2015 Oct 26. PMID: 26557808; PMCID: PMC4637345.
31. Kopher RA, Penchev VR, Islam MS, Hill KL, Khosla S, Kaufman DS. Human embryonic stem cell-derived CD34+ cells function as MSC progenitor cells. Bone. 2010 Oct;47(4):718-28. doi: 10.1016/j.bone.2010.06.020. Epub 2010 Jun 27. PMID: 20601304; PMCID: PMC2939152.

32. Lambshead JW, Meagher L, O'Brian C, Laslett AL (2013) Defining synthetic surfaces for human pluripotent stem cell culture. Cell Regeneration 2013. 2 (7) 1-15. doi:10.1186/2045-9769-2-7
33. Lian Q, Lye E, Suan Yeo K, Khia Way Tan E, Salto-Tellez M, Liu TM, Palanisamy N, El Oakley RM, Lee EH, Lim B, Lim SK. Derivation of clinically compliant MSCs from CD105+, CD24- differentiated human ESCs. Stem Cells. 2007 Feb;25(2):425-36. doi: 10.1634/stemcells.2006-0420. Epub 2006 Oct 19. PMID: 17053208.
34. Lu D, Xu Y, Zhang Q. Mesenchymal stem cell-macrophage crosstalk and maintenance of inflammatory microenvironment homeostasis. Frontiers in Cell and Developmental Biology 2021: 9:681171. doi: 10.3389/fcell.2021.681171
35. Mahmood A, Harkness L, Schrøder HD, Abdallah BM, Kassem M. Enhanced differentiation of human embryonic stem cells to mesenchymal progenitors by inhibition of TGF-beta/activin/nodal signaling using SB-431542. J Bone Miner Res. 2010 Jun;25(6):1216-33. doi: 10.1002/jbmr.34. PMID: 20200949.
36. Miura T, Yuasa N, Ota H, Habu M, Kawano M, Nakayama F, Nishihara S. Highly sulfated hyaluronic acid maintains human induced pluripotent stem cells under feeder-free and bFGF-free conditions,Biochemical and Biophysical Research Communications 2019, 518, Issue 3,Pages 506-512, https://doi.org/10.1016/j.bbrc.2019.08.082.
37. Moravcikova E, Meyer EM, Corselli M, Donnenberg VS, Donnenberg AD. Proteomic profiling of ntative unpassaged and culture expanded mesenchymal stromal cells (MSC). Cytometry Part A. 2018. 93A: 894-904.
38. Takenaka-Ninagawa, N., Kim, J., Zhao, M. et al. Collagen-VI supplementation by cell transplantation improves muscle regeneration in Ullrich congenital muscular dystrophy model mice. Stem Cell Res Ther 12, 446 (2021). https://doi.org/10.1186/s13287-021-02514-3
39. Olivier EN, Rybicki AC, Bouhassira EE. Differentiation of human embryonic stem cells into bipotent mesenchymal stem cells. Stem Cells. 2006 Aug;24(8):1914-22. doi: 10.1634/stemcells.2005-0648. Epub 2006 Apr 27. PMID: 16644919.
40. Pardue EL, Ibrahim S, Ramamurthi A. Role of hyaluronan in angiogenesis and its utility to angiogenic tissue engineering. Organogenesis. 2008 Oct;4(4):203-14. doi: 10.4161/org.4.4.6926. PMID: 19337400; PMCID: PMC2634325.
41. Peters A, Sherman LS. Diverse Roles for Hyaluronan and Hyaluronan Receptors in the Developing and Adult Nervous System. Int J Mol Sci. 2020 Aug 20;21(17):5988. doi: 10.3390/ijms21175988. PMID: 32825309; PMCID: PMC7504301.
42. Pineault N, Abu-Khader A. Advances in umbilical cord blood stem cell expansion and clinical translation. Experimental Hematology 2015; 43: 498-513.
43. Rasmusson I, Ringdén O, Sundberg B, Le Blanc K. Mesenchymal stem cells inhibit lymphocyte proliferation by mitogens and alloantigens by different mechanisms. Exp Cell Res. 2005 Apr 15;305(1):33-41. doi: 10.1016/j.yexcr.2004.12.013. Epub 2005 Jan 25. PMID: 15777785.

44. Robinson SN, Simmons PJ, Yang H, Alousi AM, Marcos de Lima J, Shpall EJ. Mesenchymal stem cells in ex vivo cord blood expansion. Best Pract Res Clin Haematol. 2011 Mar;24(1):83-92. doi: 10.1016/j.beha.2010.11.001. Epub 2011 Feb 23. PMID: 21396596; PMCID: PMC3805362.
45. Sánchez L, Gutierrez-Aranda I, Ligero G, Rubio R, Muñoz-López M, García-Pérez JL, Ramos V, Real PJ, Bueno C, Rodríguez R, Delgado M, Menendez P. Enrichment of human ESC-derived multipotent mesenchymal stem cells with immunosuppressive and anti-inflammatory properties capable to protect against experimental inflammatory bowel disease. Stem Cells. 2011 Feb;29(2):251-62. doi: 10.1002/stem.569. PMID: 21732483.
46. Sapudom J, Mohamed WKE, Garcia-Sabaté A, Alatoom A, Karaman S, Mahtani N, Teo JCM. Collagen Fibril Density Modulates Macrophage Activation and Cellular Functions during Tissue Repair. Bioengineering. 2020; 7(2):33. https://doi.org/10.3390/bioengineering7020033
47. Shen B, Wei A, Whittaker S, Williams LA, Tao H, Ma DD, Diwan AD. The role of BMP-7 in chondrogenic and osteogenic differentiation of human bone marrow multipotent mesenchymal stromal cells in vitro. J Cell Biochem. 2010 Feb 1;109(2):406-16. doi: 10.1002/jcb.22412. PMID: 19950204.
48. Simpson RM, Hong X, Wong MM, Karamariti E, Bhaloo SI, Warren D, Kong W, Hu Y, Xu Q. Hyaluronan Is Crucial for Stem Cell Differentiation into Smooth Muscle Lineage. Stem Cells. 2016 May;34(5):1225-38. doi: 10.1002/stem.2328. Epub 2016 Mar 4. PMID: 26867148; PMCID: PMC4864761.
49. Smith, R.J.P., Faroni, A., Barrow, J.R. et al. The angiogenic potential of CD271+ human adipose tissue-derived mesenchymal stem cells. Stem Cell Res Ther 12, 160 (2021). https://doi.org/10.1186/s13287-021-02177-0
50. Solis MA, Chen YH, Wong TY, Bittencourt VZ, Lin YC, Huang LL. Hyaluronan regulates cell behavior: a potential niche matrix for stem cells. Biochem Res Int. 2012;2012:346972. doi: 10.1155/2012/346972. Epub 2012 Feb 12. PMID: 22400115; PMCID: PMC3287012.
51. Stenson WF, Ciorba MA. Nonmicrobial Activation of TLRs Controls Intestinal Growth, Wound Repair, and Radioprotection. Front Immunol. 2021 Jan 21;11:617510. doi: 10.3389/fimmu.2020.617510. PMID: 33552081; PMCID: PMC7859088.
52. Su W, Matsumoto S, Sorg B, Sherman LS. Distinct roles for hyaluronan in neural stem cell niches and perineuronal nets. Matrix Biol. 2019 May;78-79:272-283. doi: 10.1016/j.matbio.2018.01.022. Epub 2018 Jan 31. PMID: 29408010; PMCID: PMC6068007.
53. Sutherland DR, Anderson L, Keeney M, Nayar R, Chin-Yee I. The ISHAGE guidelines for CD34+ cell determination by flow cytometry. International Society of Hematotherapy and Graft Engineering. J Hematother. 1996 Jun;5(3):213-26. doi: 10.1089/scd.1.1996.5.213. PMID: 8817388.
54. Toole, B. Hyaluronan: from extracellular glue to pericellular cue. Nat Rev Cancer 4, 528–539 (2004). https://doi.org/10.1038/nrc1391
55. Trivedi P, Hematti P. Derivation and immunological characterization of mesenchymal stromal cells from human embryonic stem cells. Exp Hematol. 2008 Mar;36(3):350-9. doi: 10.1016/j.exphem.2007.10.007. Epub 2008 Jan 7. PMID: 18179856; PMCID: PMC2315792.

56. Velugotla S, Pells S, Mjoseng H, Duffy CR, Smith S, De Sousa PA, Pethig R (2012) Dielectrophoresis based discrimination of human embryonic stem cells from differentiating derivatives. Biomicrofluidics 6, 044113 doi: 10.1063/1.4771316.
57. von Mering C, Jensen LJ, Snel B, Hooper SD, Krupp M, Foglierini M, Jouffre N, Huynen MA, Bork P. STRING: known and predicted protein-protein associations, integrated and transferred across organisms. Nucleic Acids Res. 2005 Jan 1;33(Database issue):D433-7. doi: 10.1093/nar/gki005. PMID: 15608232; PMCID: PMC539959.
58. Wang J, Pan W (2020) The biological role of the Collagen alpha-3 (VI) chain and its cleaved C5 domain fragment endotropin in cancer. OncoTargets and Therapy 13; 5779-93.
59. Xi H, Fujiwara W, Gonzalez K, Jan M, Liebscher S, Van Handel B, Schenke-Layland K, Pyle AD. In Vivo Human Somitogenesis Guides Somite Development from hPSCs. Cell Rep. 2017 Feb 7;18(6):1573-1585. doi: 10.1016/j.celrep.2017.01.040. PMID: 28178531; PMCID: PMC5327729.
60. Xu C, Inokuma MS, Denham J, Golds K, Kundu P, Gold JD, Carpenter MK. Feeder-free growth of undifferentiated human embryonic stem cells. Nat Biotechnol. 2001 Oct;19(10):971-4. doi: 10.1038/nbt1001-971. PMID: 11581665.
61. Xu K, Narayanan K, Lee F, Bae KH, Gao S, Kurisawa M. Enzyme-mediated hyaluronic acid-tyramine hydrogels for the propagation of human embryonic stem cells in 3D. Acta Biomater. 2015 Sep;24:159-71. doi: 10.1016/j.actbio.2015.06.026. Epub 2015 Jun 23. PMID: 26112373.
62. Yamazaki S, Hirayama R, Ikeda Y, Iseki S, Yoda T, Ikeda M-A (2023) Hyaluronic acid hydrogels support to generate integrated bone formation through endochondral ossification in vivo using mesenchymal stem cells. PLoS ONE 18(2): e0281345. https://doi.org/10.1371/journal.pone.0281345
63. Yan X, Zhou Z, Guo L, Zeng Z, Guo Z, Shao Q, Xu W. BMP7-overexpressing bone marrow-derived mesenchymal stem cells (BMSCs) are more effective than wild-type BMSCs in healing fractures. Exp Ther Med. 2018 Aug;16(2):1381-1388. doi: 10.3892/etm.2018.6339. Epub 2018 Jun 21. PMID: 30112066; PMCID: PMC6090465.
64. Zhang R, Mjoseng HK, Hoeve MA, Bauer NG, Pells S, Besseling R, Velugotla S, Tourniaire G, Kishen RE, Tsenkina Y, Armit C, Duffy CR, Helfen M, Edenhofer F, de Sousa PA, Bradley M. A thermoresponsive and chemically defined hydrogel for long-term culture of human embryonic stem cells. Nat Commun. 2013;4:1335. doi: 10.1038/ncomms2341. PMID: 23299885; PMCID: PMC3562446.
65. Zhao Q, Gregory CA, Lee RH, Lie F. MSCs derived from iPSC with a modified protocol are tumor-tropic but have much less potential to promote tumors than bone marrow MSC. PNAS 2015: 112 (2). 530-535.
66. Zöller M. CD44, Hyaluronan, the Hematopoietic Stem Cell, and Leukemia-Initiating Cells. Frontiers in Immunology. 2015 (6). DOI=10.3389/fimmu.2015.00235
67. Zwolanek D, Flicker M, Kirstätter E, Zaucke F, van Osch GJ, Erben RG. β1 Integrins Mediate Attachment of Mesenchymal Stem Cells to Cartilage Lesions. Biores Open Access. 2015 Jan

1;4(1):39-53. doi: 10.1089/biores.2014.0055. PMID: 26309781; PMCID: PMC4497673.

Figures

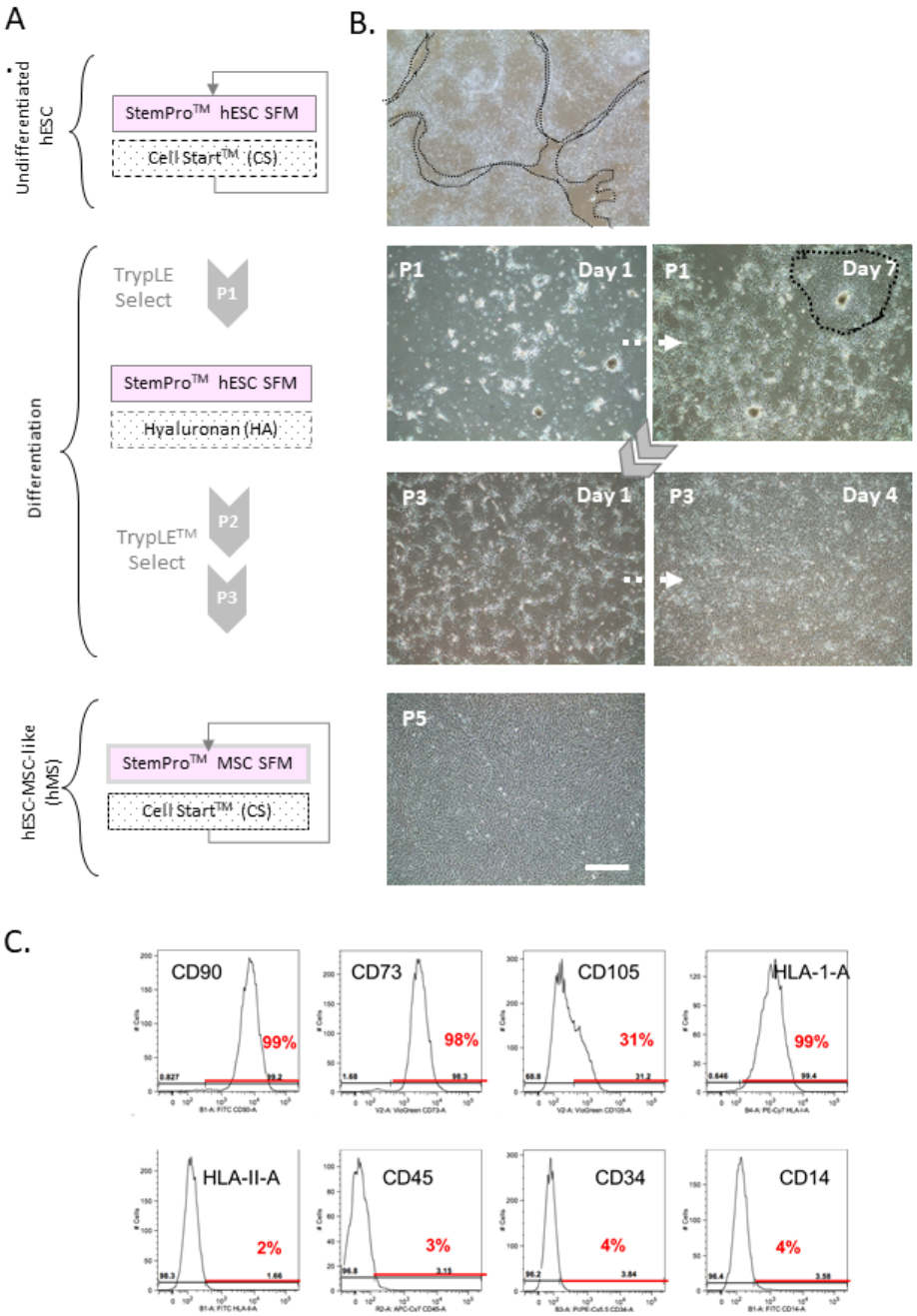

Figure 1.

Figure 1

Hyaluronan (HA) mediated differentiation of human mesenchymal stromal cell (MSC)-like cells (aka Mesenchymal Stromacytes; hMS) from human embryo stem cells (hESC). (A) Schematic overview of protocol utilising commercially available serum free media (SFM) systems for hESC and MSC serum free media culture (StemPro^{TM} hESC & MSC, respectively), substrate (CellStart^{TM}) and enzyme for cell dissociation (TrypLE^{TM} Select) over successive passages (p). (B) Representative bright field phase contrast microscopy images of cultured cells at passage number and Days post passage. Arrows denote temporal sequence. Dashed lines denote borders of undifferentiated cell colonies. Bar equals 200 µm. (C) Flow cytometry of hMS @ p19 post initiation of differentiation for MSC associated CD90, 73, 105 and HLA-I-A, and non-associated HLA-II-A, CD45, 34 and 14. Percentage of cells positive for each marker in respect of gate set for negative controls.

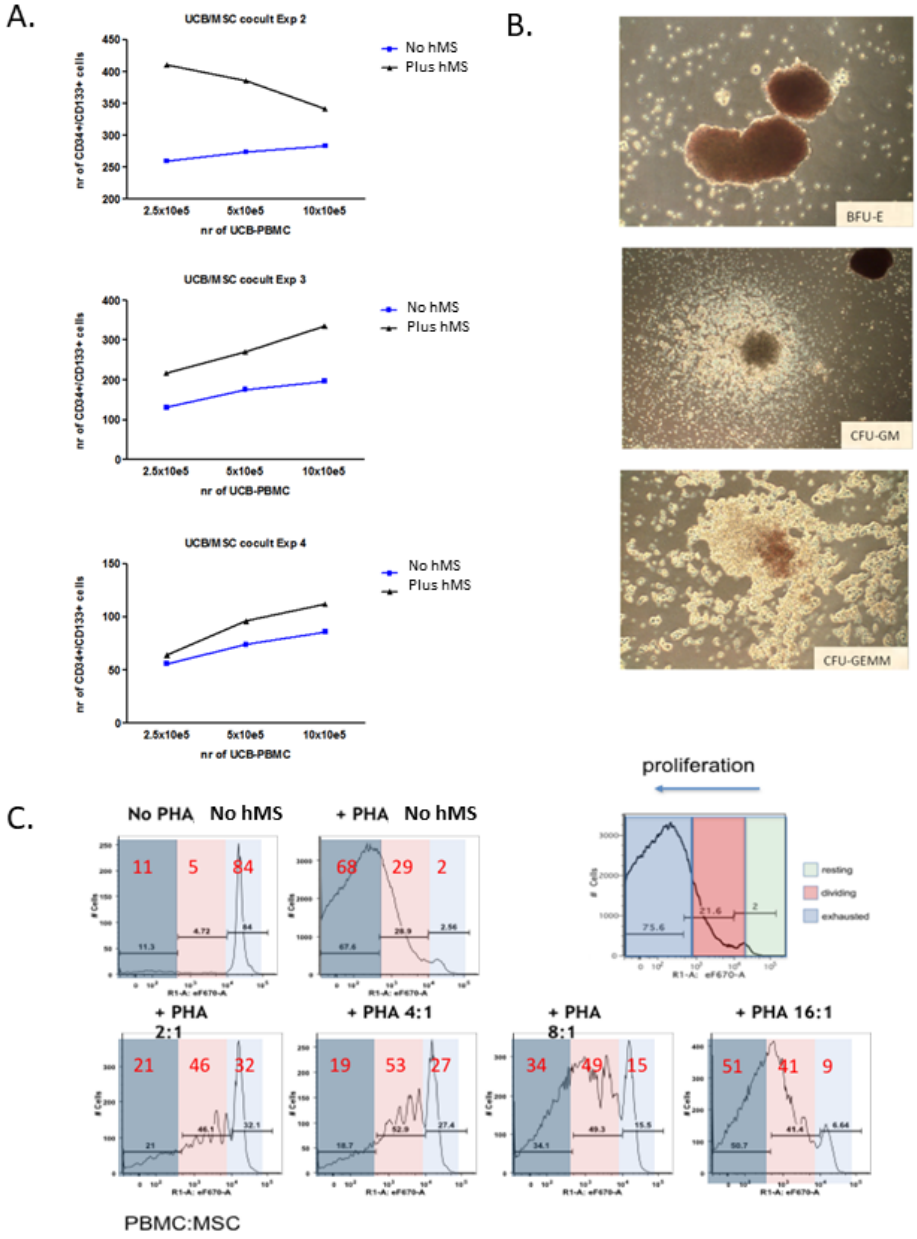

Figure 2

Figure 2

Assessment of potency of hMS co-culture to modulate primary haematopoietic progenitors and lymphocytes. (A) Yields of CD34 and CD133 double positive cells after 7 days of culture with escalating starting number of Umbilical Cord Blood- Peripheral Blood Mononuclear Cells (UCB-PBMC) with or without fixed number of hMS (MSC in figure) in defined haematopoietic progenitor medium. hMS ($1x10^6$ cells) were co-cultured with $2.5x10^5$, $5x10^5$ or $10x10^5$ cells UCB-PBN for 7 days in culture , at the end of

which the number of CD34+/CD133+ cells within the CD45+ PBMC population was determined by flow cytometry in 3 independent replications of the experimental design (exp). A total of 20000, 15000 and 5000 events were acquired for exp 1 (top), 2 (middle), and 3 (bottom), and absolute numbers of CD34+/CD133+ cells in the latter two exp were normalised to numbers in exp 1. The CD34+/CD133+ cells were quantified firstly by gating on CD45+ cells, and then on 7-Aminoactinomycin (7AAD)+ cells. **(B)** Qualitative phase contrast microscopy evidence of subsequent differentiation potency of UCB-PBMC following co-culture with hMS for Burst Forming Units of erythroid colonies (BFU-E); progression to late stage colony units of granulocyte-macrophage progenitors (CFU-GM) and granulocyte, erythrocyte, monocyte, and megakaryocytes (CFU-GEEM). **(C)** Co-culture of hMS with increasing ratio of mitogen (Phytohemagglutinin, PHA) activated adult peripheral blood mononuclear cells (PBMC) inhibits their growth in a ratio dependent manner (C). Shown is a representative outcome of two independently replicated experiment. Resting (Green/Blue), Dividing (Red) and Exhausted (Grey) cell subpopulations based on fluorescent cell tracker intensity.

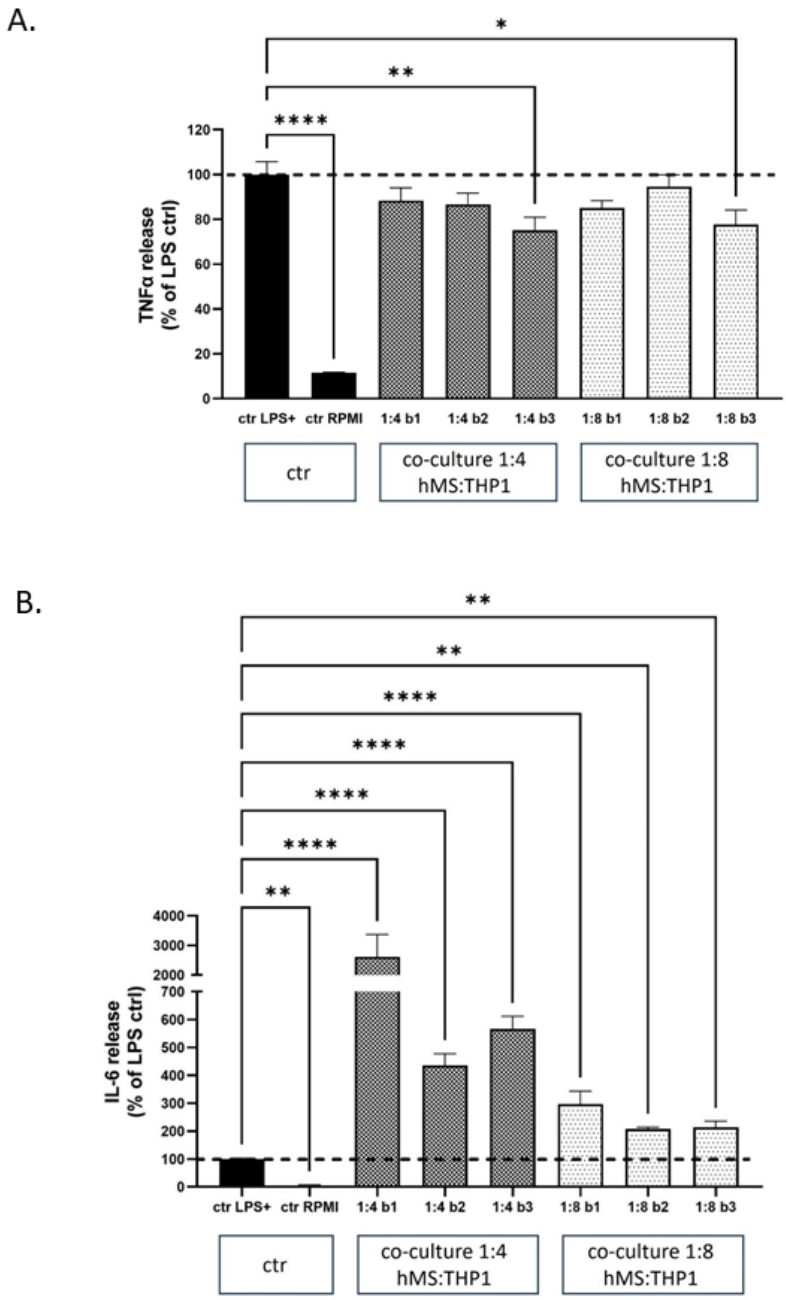

Figure 3

Figure 3

Assessment of potency of hMS co-culture to modulate inflammatory cytokine secretion from LPS stimulated THP1-M. Specifically, levels of soluble TNFα (A) and IL6 (B) in culture media were quantified by ELISAs 24 hr after LPS stimulation. Three independent batches of hMS @ p19 post HA (b1, b2, b3) were co-cultured 1:4 and 1:8 with THP1-M . In each experiment co-culture treatments and control LPS treated (ctr LPS+) and untreated in RPMI medium (ctr RPMI) were technically replicated in quadruplicate

(n=4) on the same assay plate, with cytokine levels normalized to ctr LPS+ controls, the mean of which set at 100%. Graphs depict ctr LPS+ normalized percentage mean ±standard error on the mean for each cytokine. Statistical significance of difference of level of each cytokine for each hMS batch co-culture treatment vs ctr LPS+ control was determined by one way ANNOVA and post-hoc two tailed Dunnett's multiple comparison tests. Level of significance: *<0.05; **<0.01; ****<0.0001

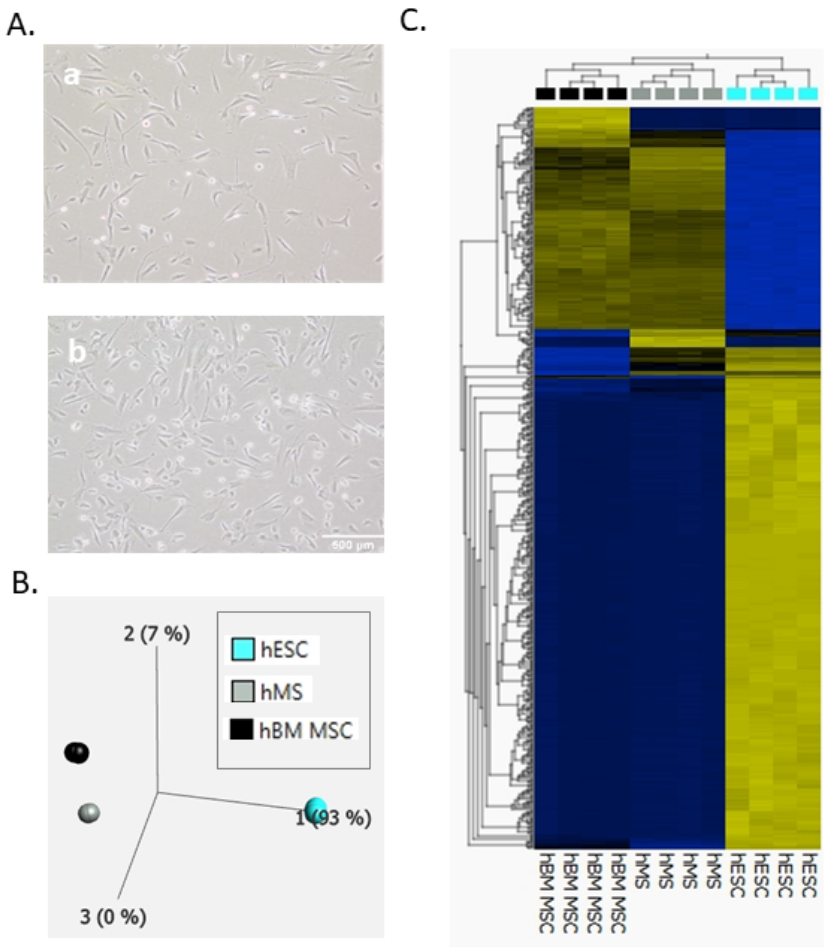

Figure 4.

Figure 4

Comparative gross cell morphology and RNA expression of hMS vs hBM-MSC and hESC. (A) Brightfield phase contrast microscopy of hBM-MSC @ p3 (a) vs hMS @ p19 post HA (b). (B) Principal component analysis and corresponding Heat Map (C) of top 500 most significant differentially expressed genes assessed by bulk cell RNAseq for aforementioned and source RC9 hESC in Stempro^{TM}-hESC SF medium on Cellstart^{TM}. Significance of p≤ 3.7379e-18 and False Discovery Rate (FDR) of q ≤ 4.2e-16

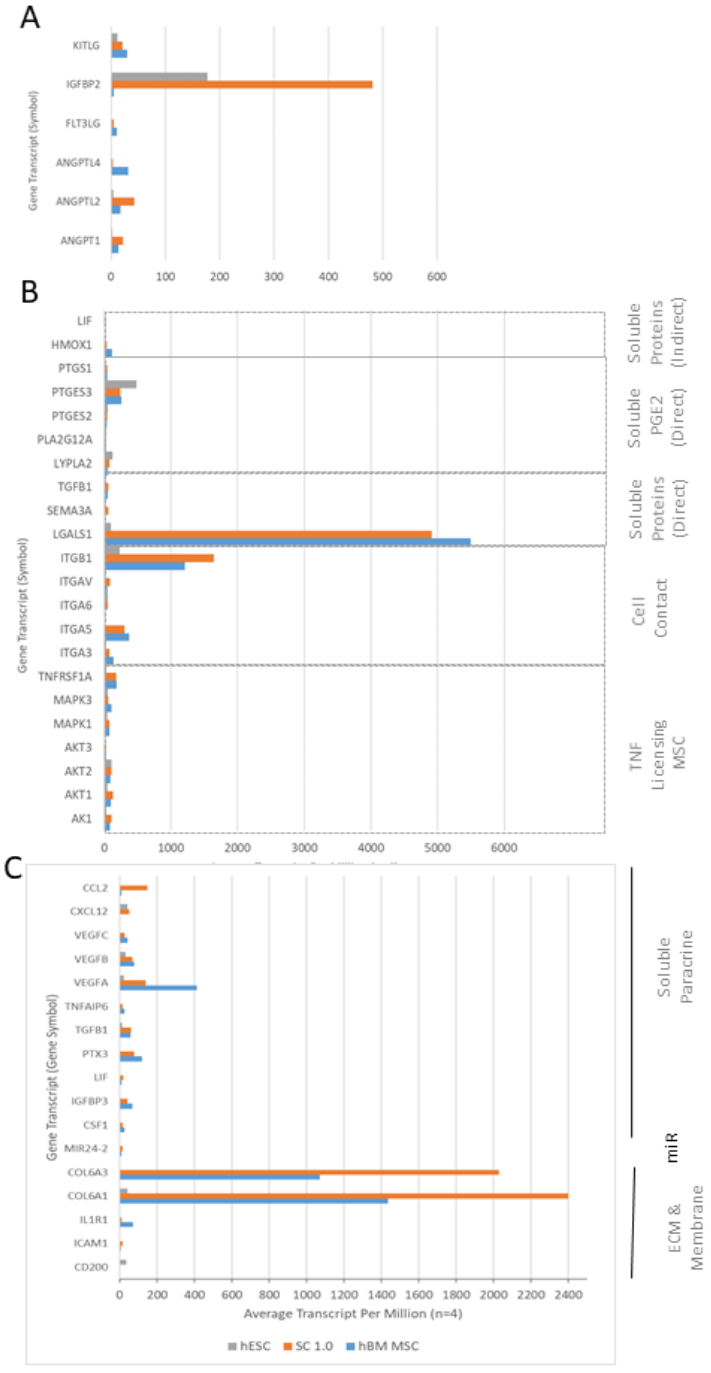

Figure 5.

Figure 5

Assessment of expression of selection of gene transcripts associated with MSC support of haematopoietic progenitor expansion (A), and adaptive immune T-cell suppression (B) and innate immune macrophage specification (C). BulkRNAseq of hBM-MSC, hESC, and hMS (in figure referred to as Stromacyte 1.0, SC1.0) assessed in excess of 196,000 RNA sequence variables identified by ENSEMBL IDs that associated with a total of 20964 genes identified by gene symbols shown in figure. Shown are Average RNA Transcript per million for selected genes for each cell type (from n=4 biological replicates for each) grouped in B & C according to form and mode of action. Gene names attributed to each symbol are: KTLG, KIT Ligand; IGFBP2, Insulin Growth Factor Binding Protein 2; FLT3LG, Fms related receptor tyrosine kinase 3 ligand; ANGPTL4, Angiopoietin like 4; ANGPTL2, Angiopoietin like 2; ANGPT1, Angiopoietin 1; LIF, Leukaemia Inhibitory Factor; HMOX1, Heme Oxygenase 1; PTGS1, Prostaglandin-endoperoxide synthase 1; PTGES3 & PTGES2: Prostaglandin E synthase 3 & 2; PLA2G12A, Phospholipase A2 group XIIA; LYPLA2, Lysophospholipase 2; TGFB1, Transforming Growth Factor Beta 1; SEMA3A, Semaphorin 3A; LGALS1, Galectin 1; ITGB1, ITGAV, ITGA6, ITGA5, ITGA3; Integrin subunit beta 1 & alpha V, 6, 5, 3; TNFRSF1A, TNF receptor superfamily member 1A; MAPK3, K1; Mitogen-activated protein kinase 3 & 1; AKT3, 2, 1; AKT serine/threonine kinase 3, 2 & 1; AK1, Adenylate kinase 1; CCL2, C-C motif chemokine ligand 2; CXCL12, C-X-C motif chemokine ligand 12; VEGFC, B, A; Vascular Endothelial Growth Factor C, B, & A; TNFAIP6, TNF alpha induced protein 6; PTX3, Pentraxin 3; IGFBP3, Insulin Growth Factor Binding Protein 3; CSF1; Colony Stimulating Factor 1; miR-24-2, MicroRNA 24-2; COL6A3 & A1, Collagen Type 6 Alpha 3 chaine & Alpha 1 chain; IL1R1, Interleukin 1 receptor type 1; ICAM1, Intercellular adhesion molecule 1; CD200, Cluster of Differentiation 200.

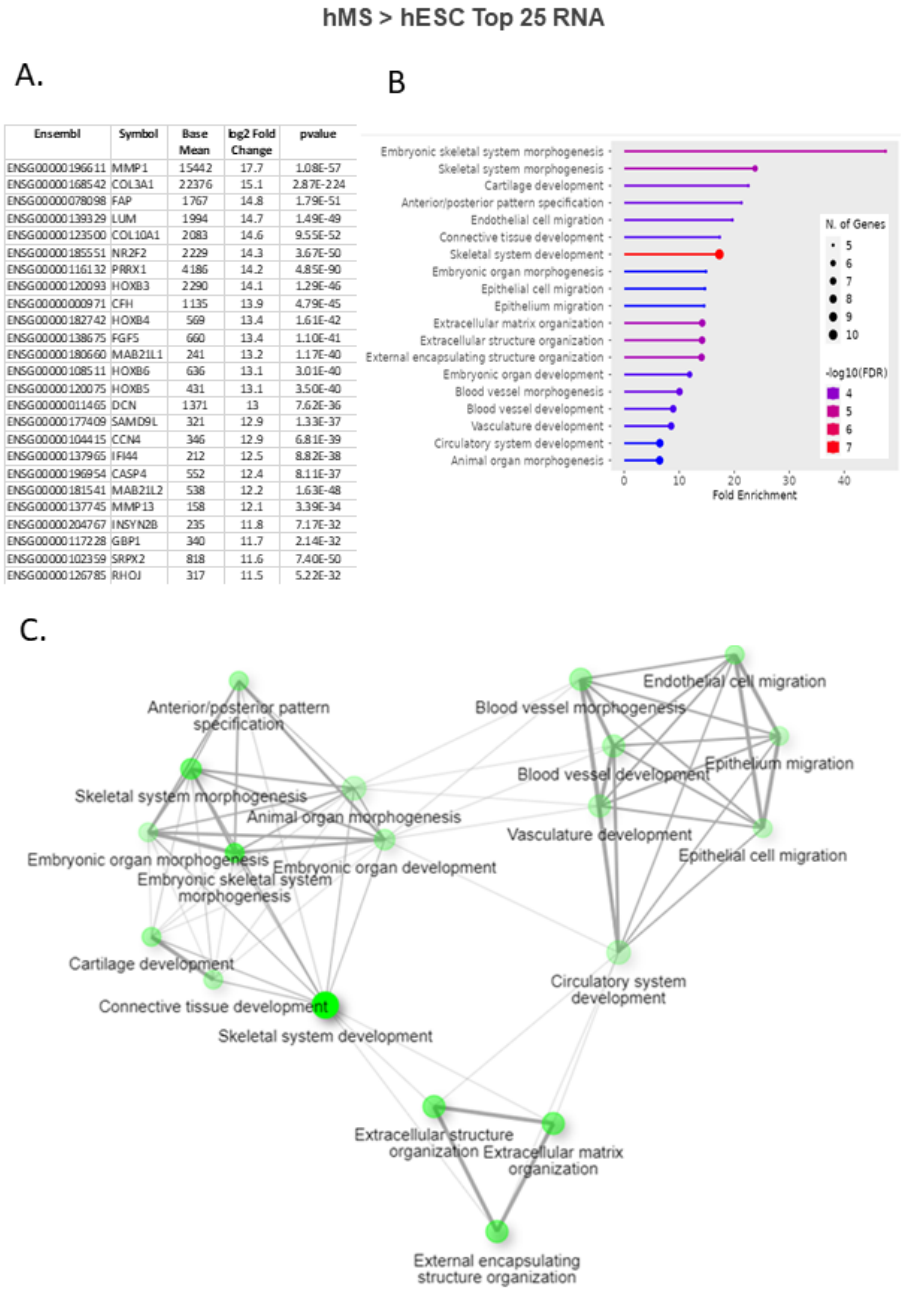

Figure 6.

Figure 6

Assessment of top 25 upregulated RNA transcripts in hMS vs hESC. (A) Tabulation of top RNA transcript variant information from left to right: Ensemble ID, Gene Symbol, Bulk RNAseq Base mean value, Log_2 fold change, and p-value. (B) ShinyGO 0.77 generated lollipop chart of top 20 Gene Ontologies (vertical axis) in relation to fold enrichment (horizontal axis) interrogating algorithm with top 25 upregulated genes. Legend: number of genes in a GO denoted by circle size and $-\log_{10}$FDR of fold enrichment for a

GO denoted by colour: blue to red, low to high. FDR, False Discovery Rate. (C) Corresponding GO network graph. Each node represents an enriched GO term, the size of the node corresponds to the number of genes and thickness of lines connecting nodes reflects percent of overlapping genes.

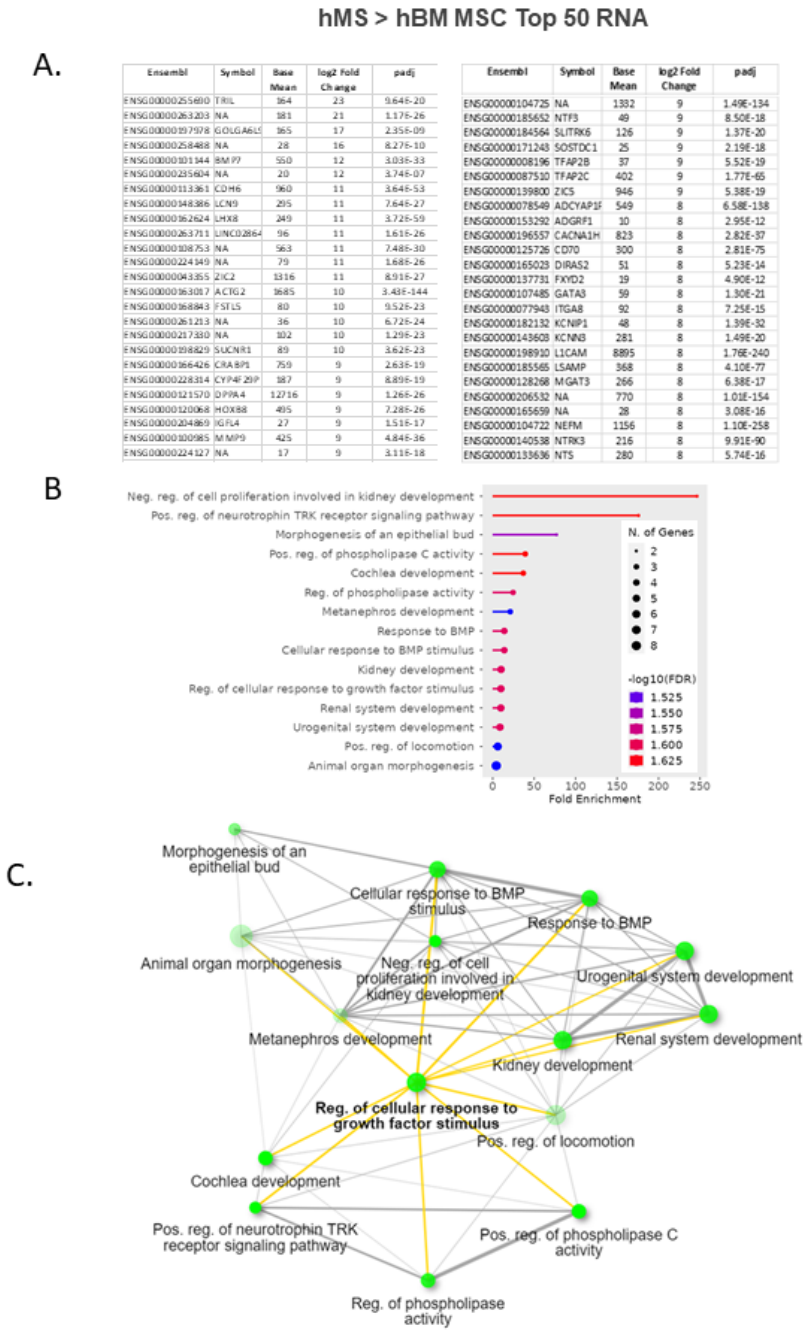

Ensembl	Symbol	Base Mean	log2 Fold Change	padj
ENSG00000255690	TRIL	164	23	9.64E-20
ENSG00000263203	NA	181	21	1.17E-26
ENSG00000197978	GOLGA6L9	165	17	2.35E-09
ENSG00000258488	NA	28	16	8.27E-10
ENSG00000101344	BMP7	550	12	3.03E-33
ENSG00000235604	NA	20	12	3.74E-07
ENSG00000113361	CDH6	960	11	3.64E-53
ENSG00000148386	LCN9	295	11	7.64E-27
ENSG00000162624	LHX8	249	11	3.72E-59
ENSG00000263711	LINC02864	96	11	1.61E-26
ENSG00000108753	NA	563	11	7.48E-30
ENSG00000224349	NA	79	11	1.68E-26
ENSG00000043355	ZIC2	1316	11	8.91E-27
ENSG00000163017	ACTG2	1685	10	3.43E-144
ENSG00000168843	FSTL5	80	10	9.52E-23
ENSG00000261213	NA	36	10	6.72E-24
ENSG00000217330	NA	102	10	1.29E-23
ENSG00000198829	SUCNR1	89	10	3.62E-23
ENSG00000166426	CRABP1	759	9	2.63E-19
ENSG00000228314	CYP4F29P	187	9	8.89E-19
ENSG00000121570	DPP4	12716	9	1.26E-26
ENSG00000120068	HOXB8	495	9	7.28E-26
ENSG00000204869	IGFL4	27	9	1.51E-17
ENSG00000100985	MMP9	425	9	4.84E-36
ENSG00000224127	NA	17	9	3.11E-18

Ensembl	Symbol	Base Mean	log2 Fold Change	padj
ENSG00000104725	NA	1332	9	1.49E-134
ENSG00000185652	NTF3	49	9	8.50E-18
ENSG00000184564	SLITRK6	126	9	1.37E-20
ENSG00000171243	SOSTDC1	25	9	2.19E-18
ENSG00000008196	TFAP2B	37	9	5.52E-19
ENSG00000087510	TFAP2C	402	9	1.77E-65
ENSG00000139800	ZIC5	946	9	5.38E-19
ENSG00000078549	ADCYAP1R1	549	8	6.58E-138
ENSG00000153292	ADGRF1	10	8	2.95E-12
ENSG00000196557	CACNA1H	823	8	2.82E-37
ENSG00000125726	CD70	300	8	2.81E-75
ENSG00000165023	DIRAS2	51	8	5.23E-14
ENSG00000137731	FKYD2	19	8	4.90E-12
ENSG00000107485	GATA3	59	8	1.30E-21
ENSG00000077943	ITGA8	92	8	7.25E-15
ENSG00000182132	KCNIP1	48	8	1.39E-32
ENSG00000143603	KCNN3	281	8	1.49E-20
ENSG00000198910	L1CAM	8895	8	1.76E-240
ENSG00000185565	LSAMP	368	8	4.10E-77
ENSG00000128268	MGAT3	266	8	6.38E-17
ENSG00000206532	NA	770	8	1.01E-154
ENSG00000165659	NA	28	8	3.08E-16
ENSG00000104722	NEFM	1156	8	1.10E-258
ENSG00000140538	NTRK3	216	8	9.91E-90
ENSG00000133636	NTS	280	8	5.74E-16

Figure 7.

Figure 7

Assessment of top 50 upregulated RNA transcripts in hMS vs hBM-MSC. (A) Tabulation of top RNA transcript variant information from left to right: Ensemble ID, Gene Symbol, Bulk RNAseq Base mean value, Log_2 fold change, and p-value. (B) ShinyGO 0.77 generated lollipop chart of top 20 Gene Ontologies (vertical axis) in relation to fold enrichment (horizontal axis) interrogating algorithm with top 50 upregulated genes. Legend: number of genes in a GO denoted by circle size and $-\log_{10}$FDR of fold enrichment for a GO denoted by colour: blue to red, low to high. FDR, False Discovery Rate. (C) Corresponding GO network graph. Each node represents an enriched GO term, the size of the node corresponds to the number of genes and thickness of lines connecting nodes reflects percent of overlapping genes. Bolded GO term and yellow highlighted connection reflects centrality of GO.

Supplementary Files

This is a list of supplementary files associated with this preprint. Click to download.

- SupplementaryTableandFigurelegends.docx
- PDSetalHAManu1SupplMaterialsSubmitted11OCT23.pptx
- AdditionalDataRNAseqTPMSubmitted11OCT23.xlsx